AMERICAN MUSEUM NOVITATES

Number 3982, 47 pp. November 8, 2021

A New Dromaeosaurid (Dinosauria: Coelurosauria) from Khulsan, Central Mongolia

JAMES G. NAPOLI,[1,2] ALEXANDER A. RUEBENSTAHL,[3] BHART-ANJAN S. BHULLAR,[3] ALAN H. TURNER,[2,4] AND MARK A. NORELL[1,2]

ABSTRACT

Dromaeosaurid theropods represent a rare but important clade of nonavialan dinosaurs. Their close evolutionary relationship to modern birds has placed them at the center of paleontological research for the last several decades. Herein we describe a new species of dromaeosaurid—*Kuru kulla*, gen. et sp. nov.—based on a partial skeleton from the Late Cretaceous Khulsan locality (Barun Goyot Formation) of Mongolia. This species is diagnosed by several autapomorphies within Dromaeosauridae, including a sharp groove anterior and ventral to the narial fossa on the premaxilla, a posterolaterally directed hornlet on the posterodorsal process of the lacrimal, a deep surangular bearing two surangular foramina, and anteriorly displaced pleurocoels on the dorsal centra. The taxon is further characterized by a unique combination of characters, including a mediolaterally narrow metatarsal II, serrations on both carinae of the dentary teeth, hyposphenes that are widely separated but joined by a web of bone, and a lacrimal with a poorly developed boss on its lateral surface. Phylogenetic analysis finds *Kuru kulla* to be the sister taxon of *Adasaurus mongoliensis*, from the slightly later Nemegt Formation, with which it is united by three synapomorphies: a posterior surangular foramen that is ~30% the depth of the surangular, absence of a fourth trochanter of the femur, and thoracic centra that are markedly longer than their midpoint widths. The recognition of this taxon has important implications for common assumptions of Mesozoic terrestrial ecosystem structure and adds new data to a recently recognized pattern in dromaeosaurid faunal composition among Late Cretaceous localities in Mongolia and Inner Mongolia (Nei Mongol Autonomous Region, China).

[1] Richard Gilder Graduate School, American Museum of Natural History, New York.
[2] Division of Paleontology, American Museum of Natural History, New York.
[3] Department of Earth & Planetary Sciences, Yale University, New Haven, CT.
[4] Department of Anatomical Sciences, Stony Brook University, Stony Brook, NY.

 ISSN 0003-0082

INTRODUCTION

Despite their overall rarity in the fossil record, dromaeosaurid dinosaurs are among the best-represented and best-studied paravian theropods. Dromaeosaurids were central to the recognition of modern birds as living dinosaurs, which was spurred by the discovery of *Deinonychus antirrhopus* (then the most completely known dromaeosaurid), a taxon that preserved many characteristically "avian" traits in its postcranial skeleton (Ostrom, 1969a). Several exceptional dromaeosaurid specimens from the American Museum of Natural History–Mongolian Academy of Sciences (AMNH-MAS) expeditions to the Gobi provided important new data including characters of the pectoral girdle, forelimb, pelvis, and pes, which further refuted arguments against a dinosaur origin of birds (Norell and Makovicky, 1997, 1999). The discoveries of the small-bodied dromaeosaurids *Microraptor zhaoianus* and *Sinornithosaurus millenii* (Xu et al., 1999, 2000), and the recognition of feather quill knobs on a eudromaeosaur specimen (Turner et al., 2007a), demonstrated conclusively that dromaeosaurid dinosaurs were fully feathered. *Microraptor* in particular has featured prominently in research regarding the origin(s) of flight in Paraves (Pei et al., 2020).

Irrespective of their direct relevance to contextualizing the origin of modern birds, dromaeosaurids have proven to be an exceptionally diverse group of nonavian theropods. Discoveries in the past three decades has led to an exponential increase in our knowledge of the diversity of this clade. Ancestrally, dromaeosaurids were small-bodied and likely nonpredatory animals (Turner et al., 2007b; Cau et al., 2017), which later achieved a wide array of body plans and diets (Napoli et al., in review), represented by long-snouted unenlagiines, small and potentially volant microraptorines, and macropredatory eudromaeosaurs (Makovicky et al., 2005; Turner et al., 2012; Pei et al., 2020). Of these clades, eudromaeosaurs are the best represented, with specimens known from Europe, Asia, and North America testifying to a diverse radiation of mostly small to midsized terrestrial predators (Turner et al., 2012; Pittman et al., 2020). Exceptional eudromaeosaur fossils provide potential evidence of pack hunting and demonstrate that these animals habitually predated upon prey larger than themselves (Maxwell and Ostrom, 1995; Barsbold and Osmólska, 1999; Li et al., 2008).

The best eudromaeosaur fossils come from the Gobi Desert, particularly from Late Cretaceous localities in Inner Mongolia (Nei Mongol Autonomous Region, China) and Mongolia, which have produced remains of *Velociraptor mongoliensis* (Osborn, 1924), *Adasaurus mongoliensis* (Barsbold, 1983), *Achillobator giganticus* (Perle et al., 1999), *Tsaagan mangas* (Norell et al., 2006), *Velociraptor osmolskae* (Godefroit et al., 2008), *Linheraptor exquisitus* (Xu et al., 2010), and *Shri devi* (Turner et al., 2021). Recent phylogenetic analyses (Pei et al., 2020; Turner et al., 2021; Napoli et al., in review) have found all Late Cretaceous Asian eudromaeosaurs except *Achillobator* to comprise the clade Velociraptorinae, also including *Deinonychus antirrhopus* and potentially several fragmentary North American eudromaeosaurs. Here, we report a new species of eudromaeosaur from the Late Cretaceous Khulsan locality, from which one eudromaeosaurid taxon – *Shri devi* – is currently recognized (Turner et al., 2021). This new taxon is represented by a partial skeleton that preserves strong character support for its taxonomic distinctiveness and membership within the clade Velociraptorinae. The presence of two similarly sized, closely related taxa in one locality has implications for our understanding of, and assumptions regarding, the composition of other Mesozoic faunas.

SYSTEMATIC PALEONTOLOGY

Dinosauria Owen, 1843

Theropoda Marsh, 1881

Coelurosauria Huene, 1920

Maniraptora Gauthier, 1986

Dromaeosauridae Matthew and Brown, 1922

Kuru kulla, gen. et sp. nov

ETYMOLOGY: Kurukullā (fig. 1) is a deity venerated in Tibetan Buddhism. Considered peaceful to semiwrathful, she is usually depicted with four arms, holding in one pair of hands a bow and arrow, and in the other pair a hook and noose, all of which are made of flowers. Kurukullā is particularly associated with major life transitions. We emphasize here that the generic name *Kuru* is *not* in reference to the cannibalism-borne prion disease of the same name.

HOLOTYPE: IGM 100/981, a fragmentary skeleton comprising a right premaxilla, right lacrimal, partial right dentary, right surangular, 14 presacral vertebrae, three caudal vertebrae, fragments of the right and left upper limb, a fragmentary ilium, distal ends of both pubes, right and left femora, a right tibia, and fragments of the right and left pes.

TYPE LOCALITY: Khulsan (fig. 2). The Barun Goyot Formation crops out at the Khulsan locality, and is lithologically similar to the sandstones of the Djadokhta Formation (Turner et al., 2021). Efforts to determine the relative ages of Djadokhta and Djadokhta-like strata and localities (such as Ukhaa Tolgod, Bayn Dzak, Kheermen Tsav, and Bayan Mandahu) have been stymied by a lack of precise geochronological data and observable contacts (Dingus et al., 2008). All that can be said with certainty is that the Barun Goyot strata at Khulsan are Campanian to Maastrichtian in age. Some taxa, such as the oviraptorid *Nemegtomaia barsboldi*, are reported from the Barun Goyot and Nemegt formations, but others (such as the lizard *Estesia mongoliensis*; Yi and Norell, 2013) are shared with Djadokhta-equivalent formations, possibly suggesting that the Barun Goyot Formation is intermediate in age between the Djadokhta and Nemegt Formations. However, as all three localities continue to yield new taxa, it is equally possible that some are contemporaneous and that more overlapping taxa remain undiscovered.

DIAGNOSIS: Dromaeosaurid theropod distinguishable from other Late Cretaceous dromaeosaurids by the following combination of characters (putative autapomorphies within Dromaeosauridae are denoted with an asterisk): deeply incised groove framing the anterior and ventral margins of the narial fossa on the premaxilla*; lacrimal with posterolateral hornlet arising from the posterodorsal process*, lacrimal with poorly developed boss at intersection of ventral, posterodorsal, and anterior processes, dentary lacking a ventral secondary row of nutrient foramina, dentary nutrient foramina set in a shallow groove posteriorly, dentary teeth serrated on both the mesial and distal carinae, two posterior surangular foramina*, proportionally deep surangular*, anteriorly displaced (rather than anteroposteriorly centered) pleurocoels on dorsal centra*, hyposphenes widely separated and joined by a web

FIGURE 1. Tangka depicting Kurukullā from the Hall of Asian Peoples, American Museum of Natural History.

of bone, distal tarsals unfused to metatarsus, mediolaterally narrow metatarsal II, relatively reduced pedal digit II.

Note on Holotype Specimen: To avoid future confusion regarding the proper number for the holotype specimen of *Kuru kulla* we provide here a brief history of published references to this specimen, as well as a past erroneous application of this specimen number to a different dromaeosaurid specimen from the Gobi. A partial dromaeosaurid specimen from Khulsan was referred to as IGM 100/981 in the "important features" papers (Norell and Makovicky, 1997, 1999), and the surangular

FIGURE 2. Map of Mongolia, showing the location of Khulsan, the locality in which IGM 100/981 was discovered in 1991.

of this same individual was figured and labeled as IGM 100/981 by Norell et al. (2006: fig. 15). It is this specimen cataloged as IGM 100/981 that we describe and name herein. This specimen may further be familiar (erroneously) under the provisional name "*Airakoraptor*," which was listed in a table by Perle et al. (1999) in their description of *Achillobator giganticus*, a paper published without the knowledge of its junior authors and based on written material left in Mongolia (Turner et al., 2012). The name is referenced to a Society of Vertebrate Paleontology meeting abstract, albeit with an incorrect title, and may derive from a fermented mare- or donkey-milk product called "airak" that is important in traditional Central Asian steppe culture (also spelled "airag" in Mongolian and often referred to in English by the Kazakh word "kumis"). As IGM 100/981 was never actually described as "*Airakoraptor*," the name is a nomen nudum.

An incomplete dromaeosaurid specimen from Zos Wash (near Ukhaa Tolgod) was collected in 1998 (a year after IGM 100/981 appeared in the literature). This specimen is notable for its preservation of ulnar papillae, which are the first direct evidence of feathers in a eudromaeosaur (Turner et al., 2007a). The Zos Wash specimen was also mentioned by Norell et al. (2006), who noted that it was not referrable to *Tsaagan mangas* due to differences in frontal morphology, despite shared provenance. Turner et al. (2007a) erroneously identified the Zos Wash specimen as IGM 100/981. The correct specimen number for the Zos Wash specimen is IGM 100/3503. This individual is currently referred to *Velociraptor mongoliensis* and is under renewed study.

Institutional Abbreviations

AMNH FARB, American Museum of Natural History Fossil Amphibians, Reptiles, and Birds, New York
IGM, Mongolian Institute for Geology, Ulaanbaatar, Mongolia
YPM, Yale Peabody Museum of Natural History, New Haven, CT
ZPAL, Institute of Paleobiology, Polish Academy of Sciences, Warsaw, Poland

DESCRIPTION

IGM 100/981 comprises a partial skeleton, including a right premaxilla and lacrimal, a right partial mandible, parts of 14 presacral vertebrae, three isolated caudal vertebrae, and fragments of the left and right fore- and hind limbs. Preservational quality differs among elements, but generally the elements are more heavily weathered than those of the recently described holotype of the dromaeosaurid *Shri devi* (Turner et al., 2021).

Cranium

The cranium of IGM 100/981 is represented only by a partial right premaxilla and partial right lacrimal. The medial surface and part of the dentigerous margin of the premaxilla (fig. 3) are obscured by matrix. Only the first two alveoli are exposed, precluding a definite dental count, but there were almost certainly four premaxillary teeth, as in all theropods. The anterior and ventral margins of the premaxilla meet at an approximately 90° angle, as in all dromaeosaurids. The anteroventral end is marked by irregularly arranged neurovascular foramina, like those of *Velociraptor mongoliensis* (AMNH FARB 6515; IGM 100/982). The nasal process is incomplete, precluding observations of its posterior morphology, but it was clearly rounded, as is typical for dromaeosaurids, rather than externally flattened as in troodontids. The subnarial process is broken at its anterior base, so it cannot be determined whether it extended posteriorly to exclude the maxilla from the margin of the external naris. However, this is the most likely condition, as it is known in all eudromaeosaurs for which the relevant anatomy is preserved. Ventral to the base of the subnarial process is a posteroventrally facing fossa that represents the premaxillary contribution to the subnarial foramen, which would have opened between the maxilla and premaxilla as in most theropods. In *Deinonychus antirrhopus* (YPM 5232) there is no clear fossa for this foramen on the lateral surface of the premaxilla ventral to the subnarial process, and the anterior end of the maxilla is reconstructed, so the presence of a subnarial foramen is unclear. The narial fossa extends onto the base of the nasal process. Anterior to the narial fossa, there is a conspicuous groove roughly paralleling its anterior margin. Dorsally, this groove terminates in a distinct, sediment-infilled neurovascular foramen, and posteriorly/ventrally it appears to enter the subnarial foramen. A similar groove is present in *Tsaagan mangas* (IGM 100/1015) and appears to be present in both *Linheraptor exquisitus* (Xu et al., 2015, fig. 4A; IVPP V 16923) and *Velociraptor mongoliensis* (IGM 100/982); however, it is more weakly developed in all three taxa than it is in IGM 100/981. A similar shallowly inset groove appears to be present in *Velociraptor mongoliensis*

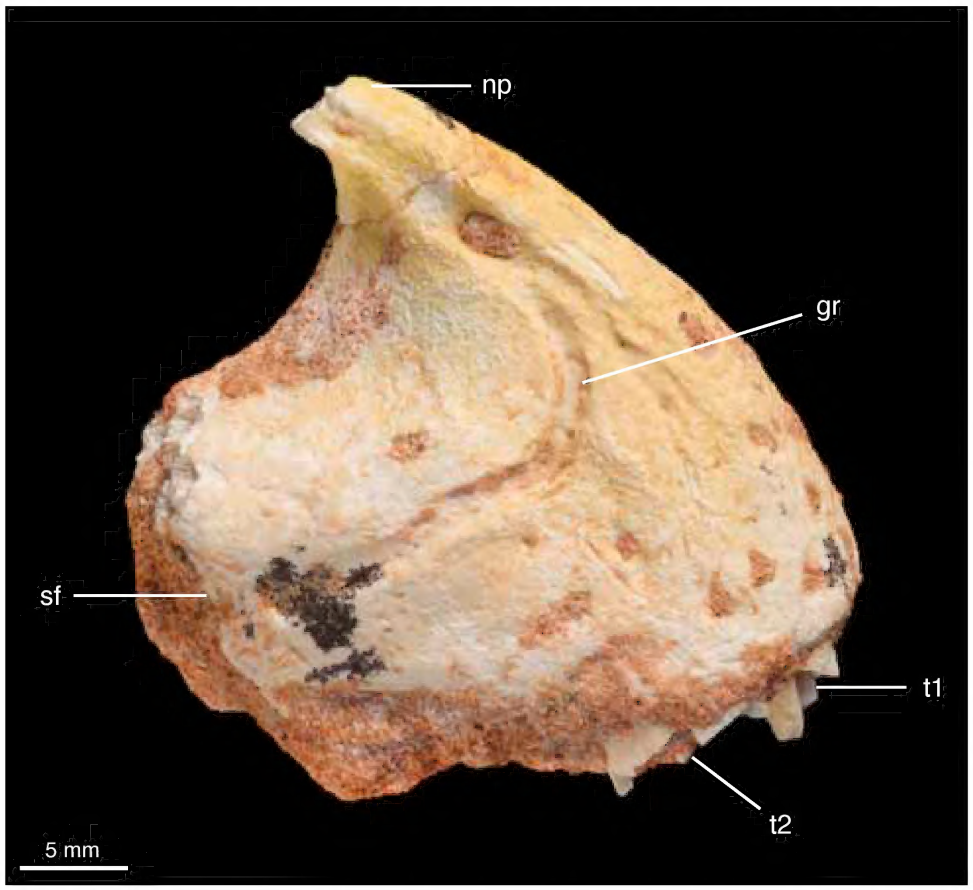

FIGURE 3. Right premaxilla of IGM 100/981 in lateral view. Abbreviations: **gr,** groove anterior to narial fossa; **np,** nasal process; **sf,** premaxillary contribution to subnarial foramen; **t1,** first premaxillary tooth; **t2,** second premaxillary tooth.

(AMNH FARB 6515), although in this specimen it is wider, oriented vertically, and extends farther dorsally and ventrally. There is an enlarged neurovascular foramen at the base of the subnarial process, which is smaller than the one found in the same position in *Deinonychus antirrhopus* (YPM 5232).

The lacrimal is missing its anterior half, so the entire anterior process and most of the ventral process are missing (fig. 4). However, the posterodorsal process is preserved and nearly complete, indicating that IGM 100/981 had a typical dromaeosaurid T-shaped lacrimal. The posterodorsal process is triangular in IGM 100/981, unlike the deeper posterodorsal process of the lacrimal in *Velociraptor mongoliensis* (IGM 100/982). It is impossible, however, to determine the relative lengths of the anterior and posterodorsal processes. The preserved portion of the ventral process indicates that it was vertically oriented. Medially, the anterior portion of the preserved lacrimal retains the articular surface for the nasal. It forms a small shelf underlying the nasal anteriorly, which grades into the body of the lacrimal posteriorly as a dorsal shelf arises from it. Therefore, the lacrimal transitions from underlying the nasal anteriorly to overlying it posteriorly. The shelf for the nasal persists to at least the midpoint of the posterior process

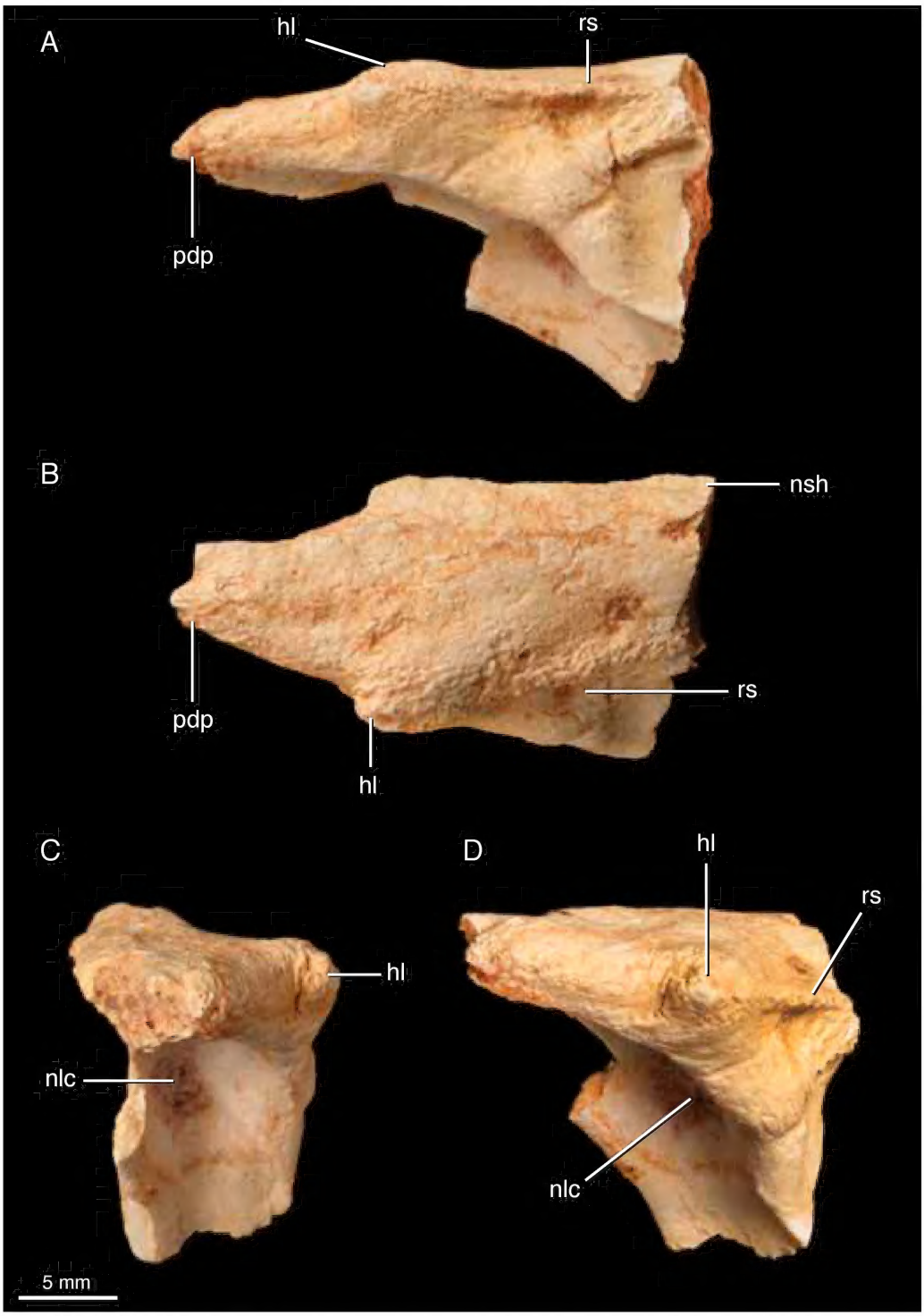

FIGURE 4. Right lacrimal of IGM 100/981 in **A,** lateral, **B,** dorsal, **C,** posterior, and **D,** posterolateral views. Abbreviations: **hl,** orbital hornlet; **nlc,** nasolacrimal canal; **nsh,** shelf underlying nasal; **rs,** rugose shelf overhanging ventral process; **pdp,** posterodorsal process.

of the lacrimal, which is substantially farther than the shelf persists in *Deinonychus antirrhopus* (YPM 5232) and *Velociraptor mongoliensis* (IGM 100/982), in which it terminates at about the anterior edge of the ventral process of the lacrimal. The articular surface for the frontal is damaged, so it is impossible to determine whether it had a distinct notch. Laterally, the dorsolateral edge of the lacrimal is rugose and forms a sharp rugose ridge slightly overhanging the ventral process. This ridge inflates posteriorly, forming a rugose, posteriorly directed hornlet. Several dromaeosaurids, including *Tsaagan mangas* (IGM 100/1015), *Linheraptor exquisitus* (Xu et al., 2015; IVPP 16923), *Velociraptor mongoliensis* (IGM 100/976; IGM 100/982; AMNH FARB 6515), and *Deinonychus antirrhopus* (YPM 5232), have a rugose boss on the lateral surface of the lacrimal at the intersection of the anterior, posterodorsal, and jugal processes. In IGM 100/981, however, this lacrimal boss is represented only by a small, smooth swelling. Posteriorly, this rugose hornlet grades into the orbital margin of the posterodorsal process of the lacrimal, which is smooth in texture. Ventrally, the posterodorsal process is dotted with small neurovascular foramina, which are also seen in *Deinonychus antirrhopus* (YPM 5232), *Tsaagan mangas* (IGM 100/1015), and sparsely in *Velociraptor mongoliensis* (AMNH FARB 6515). The ventral process of the lacrimal is deeply excavated posteriorly to form the anterodorsal margin of the orbit. A patch of infilled sediment appears to mark the posterior opening of the nasolacrimal canal, which transmitted the nasolacrimal duct in life. The opening for this duct is more circular than in *Deinonychus antirrhopus* (YPM 5232) in which the canal is almost slit-like, but is similar to the opening in *Velociraptor mongoliensis* (AMNH FARB 6515; IGM 100/982).

Mandible

The left mandible of IGM 100/981 is present in four pieces comprising a nearly complete left dentary and surangular. As in many dromaeosaurids, including *Shanag ashile* (IGM 100/1119), the anterior end of the dentary is downturned (fig. 5), such that the first dentary tooth is slightly prognathous. The dentary is straplike, as in all dromaeosaurids but unlike troodontids and avialans, and is straight along its length, unlike the dorsoventrally bowed dentaries of *Acheroraptor temertyorum* (AMNH FARB 32108; Evans et al., 2013), *Tsaagan mangas* (IGM 100/1015), and *Velociraptor mongoliensis* (AMNH FARB 6515; IGM 100/982) but like that of *Dromaeosaurus albertensis* (AMNH FARB 5356) and *Deinonychus antirrhopus* (YPM 5232). The anterior end of the dentary is marked by numerous, irregularly arranged nutrient foramina. As in *Shanag ashile* (IGM 100/1119), *Acheroraptor temertyorum* (AMNH FARB 32108; Evans et al., 2013), *Tsaagan mangas* (IGM 100/1015), and *Velociraptor mongoliensis* (AMNH FARB 6515; IGM 100/982), but unlike *Dromaeosaurus albertensis* (AMNH FARB 5356), the primary nutrient foramina on the dentary lie in a shallow groove posteriorly. Unlike *Shanag ashile* (IGM 100/1119) and many eudromaeosaurs, such as *Saurornitholestes langstoni* (Currie and Evans, 2019), *Acheroraptor temertyorum* (AMNH FARB 32108; Evans et al., 2013), *Tsaagan mangas* (IGM 100/1015), *Velociraptor mongoliensis* (AMNH FARB 6515; IGM 100/982), and *Deinonychus antirrhopus* (YPM 5232) but similar to *Dromaeosaurus albertensis* (AMNH FARB 5356), there is no secondary row

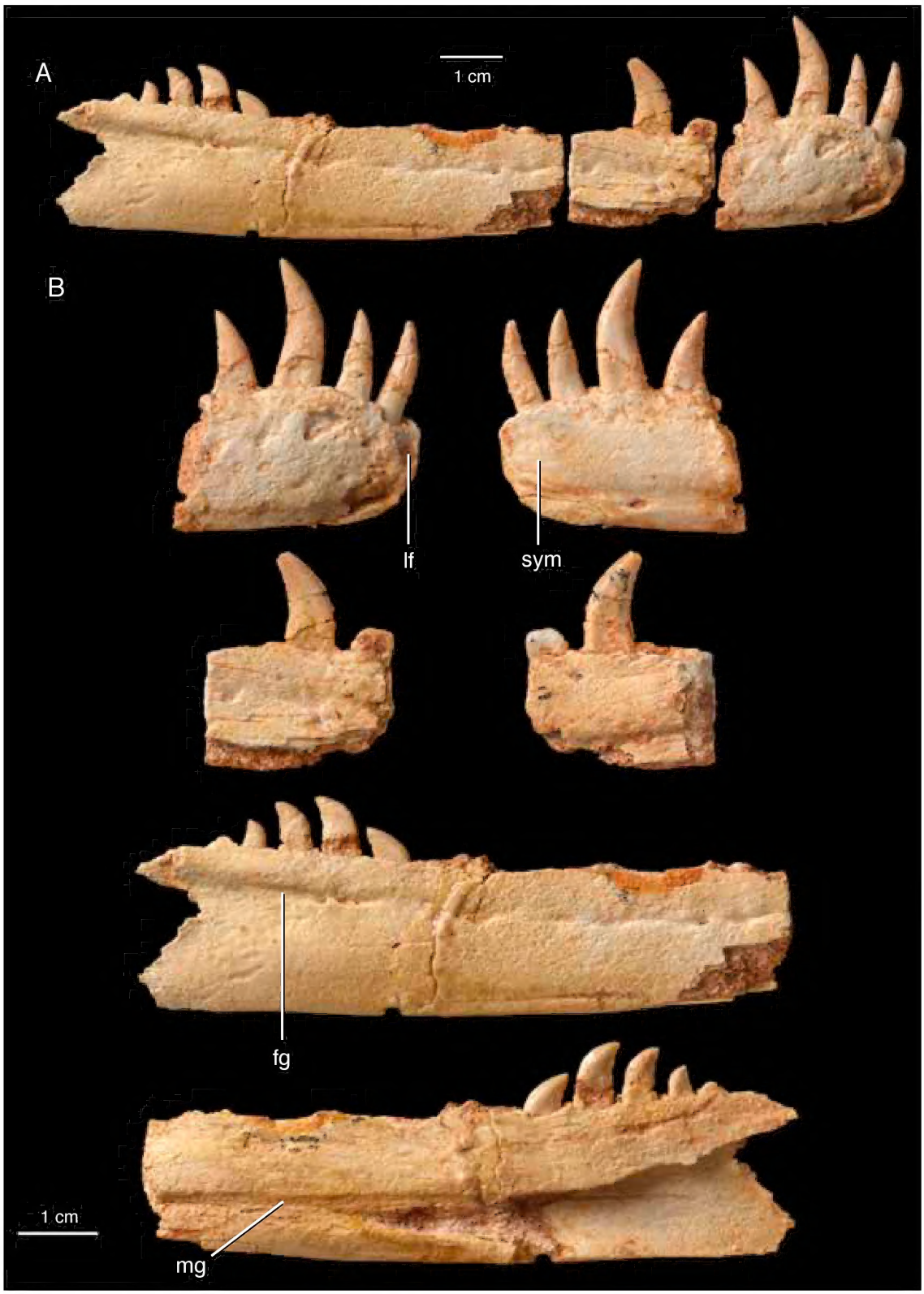
A
1 cm
B
lf
sym
fg
1 cm
mg

of nutrient foramina near the ventral margin of the dentary. Like *Saurornitholestes langstoni* (Currie and Evans, 2019), *Velociraptor mongoliensis* (AMNH FARB 6515; IGM 100/982), *Acheroraptor temertyorum* (AMNH FARB 32108; Evans et al., 2013), *Dromaeosaurus albertensis* (AMNH FARB 5356), *Tsaagan mangas* (IGM 100/1015), and *Atrociraptor marshalli* (Currie and Evans, 2019), there is a large, anterodorsally open foramen at the anterior tip of the dentary. In *Deinonychus antirrhopus* (YPM 5232; YPM 5210), at the most anterior tip of the dentary, there is instead an enlarged foramen on the lateral surface that directs anterolaterally. There is no indication of a ventral "chin," which is not seen in any dromaeosaurids but is common in tyrannosaurids (Brusatte et al., 2010). The anterior edge of the dentary in IGM 100/981 is steep like in *Velociraptor mongoliensis* (AMNH FARB 6515), with much of the anterior edge vertical and the edge of the dentary rounded, unlike *Deinonychus antirrhopus* (YPM 5232) in which the anterior edge of the dentary slopes gradually posteroventrally making the tip acutely pointed. The dentary bears no fewer than 14 tooth positions, and possibly up to 15. This is large in comparison to several eudromaeosaurs such as *Acheroraptor temertyorum* (AMNH FARB 32108) and *Bambiraptor feinbergi* (AMNH FARB 30556), which both preserve 12 dentary tooth positions, and *Dromaeosaurus albertensis* (AMNH FARB 5356), which has 11. However, this is similar to the dentary tooth count of 15 in *Saurornitholestes langstoni* (Currie and Evans, 2019) and *Deinonychus antirrhopus* (YPM 5232; YPM 5210), and of 14 in *Tsaagan mangas* (IGM 100/1015) and *Velociraptor mongoliensis* (AMNH FARB 6515; IGM 100/982). The dentary tooth positions are equally spaced, with no indication of closely packed teeth in the anterior dentary as seen in troodontids and basal dromaeosaurids. Anteriorly, there is no concave notch in the ventral margin as in *Saurornitholestes langstoni* (Currie and Evans, 2019). As in all dromaeosaurids, there is no indication of interdental plates on the medial dentary (contra Currie, 1995; contra Evans et al., 2013). The symphyseal region of the dentary is smooth, lacking any texturing for ligament attachment. The Meckelian groove is shallow and dorsoventrally broad, and located ventrally on the dentary, similar to *Tsagaan mangas* (IGM 100/1015) and *Velociraptor mongoliensis* (AMNH FARB 6515), though it does not extend as far anteriorly as in the latter. It is more shallowly inset than that of *Acheroraptor temertyorum* (AMNH FARB 5356), in which the Meckelian groove is deeper overall and deepens posteriorly. While the Meckelian groove is similar in depth to that in *Deinonychus antirrhopus* (YPM 5232; YPM 5210), the dorsal edge of the groove overhangs the ventral edge, which is unlike the condition in *Deinonychus* (YPM 5232; YPM 5210) and *Velociraptor mongoliensis* (AMNH FARB 6515). The depth of the Meckelian groove also appears to differ between specimens of *Deinonychus antirrhopus* of different sizes, with smaller *Deinonychus antirrhopus* (YPM 5232) having a shallower groove than larger individuals (YPM 5210), raising the possibility that this structure is allometrically or ontogenetically variable in dromaeosaurids.

The surangular (fig. 6) in IGM 100/981 is distinctive in its dorsoventral depth (contrasting the dorsoventrally shallow surangular in other dromaeosaurids) and in possessing two, rather than one, posterior surangular foramina, a condition unique to this taxon among known drom-

FIGURE 5. Right dentary of IGM 100/981, showing **A,** all fragments in life position, in lateral view, and **B,** each fragment in lateral (left) and medial (right) view. Abbreviations: **fg,** foraminal groove; **lf,** large nutrient foramen; **mg,** Meckelian groove; **sym,** symphyseal surface.

aeosaurids. The surangular of the potentially chimeric *Bagaraatan ostromi* also possesses two posterior surangular foramina (in which one partially overlies the other dorsally, unlike in IGM 100/981; Osmólska, 1996), as does the troodontid *Sinornithoides youngi* (Russell and Dong, 1993). While *Saurornitholestes langstoni* possesses two surangular foramina (Currie and Evans, 2019), its accessory anterior foramen is positioned anterior to the surangular shelf, above the external mandibular fenestra. Thus, it is not homologous to either of the surangular foramina seen in IGM 100/981. A second surangular foramen was reported as ambiguously present on the right side in *Tsaagan mangas* near the quadrate articulation (Norell et al., 2006), but it is not present in the possibly synonymous *Linheraptor exquisitus* (Xu et al., 2010, 2015) and is not apparent in CT scans. Combined with firsthand reexamination of IGM 100/1015 we conclude that *Tsaagan mangas* lacks this structure. The more anterior of the two surangular foramina of IGM 100/981 (here interpreted as the homolog of the single surangular foramen of most theropods) is large, approximately 28% of the dorsoventral depth of the surangular at its midpoint and is larger than, but comparable to, that of *Tsaagan mangas* (IGM 100/1015) and *Velociraptor mongoliensis* (IGM 100/982). This is smaller than the extremely large surangular foramen of *Adasaurus mongoliensis* (Turner et al., 2012), but is larger than that of most other theropods including most dromaeosaurids, especially *Deinonychus antirrhopus*, in which it is very small. The posterior foramen is about half the size of the anterior. Both foramina are overhung by a dorsolaterally projecting surangular shelf, which does not abut the dorsal margins of the foramina and does not obscure them from lateral view. Together with a strong medial ridge, the surangular shelf forms a dorsally facing surface for attachment of the *M. adductor mandibulae* musculature. In most dromaeosaurids, including *Dromaeosaurus albertensis* (AMNH FARB 5356), *Tsaagan mangas* (IGM 100/1015) and *Velociraptor mongoliensis* (AMNH FARB 6515), the surangular shelf projects laterally, is more weakly developed, or both, and this muscle-attachment surface correspondingly faces dorsolaterally. While not as well developed in YPM 5234, *Deinonychus antirrhopus* and one specimen of *Velociraptor mongoliensis* (IGM 100/982) have a more dorsally inclined surangular shelf, similar to that of IGM 100/981. As in *Deinonychus antirrhopus* (YPM 5234) there is a short dorsal triangular process on the posterior portion of the surangular that likely contributed to the lateral edge of the posterior rim of the glenoid fossa, which is not as tall as the process in *Tsaagan mangas* (IGM 100/1015) and *Deinonychus antirrhopus* (YPM 5234). Though the posterior edge of the surangular is partially broken, the medial surface of the surangular preserves the articular surface for the articular. As in *Deinonychus antirrhopus* (YPM 5234) the articular projected anteroventrally, along the ventral edge of the medial surface of the surangular and narrowing anteriorly.

Dentition

The dentition of IGM 100/981 is represented by teeth preserved in situ in the left dentary (fig. 5), as well as three isolated maxillary or dentary teeth. The teeth are ziphodont in shape (sensu Hendrickx et al., 2015), as in all derived dromaeosaurids, with long roots like those of

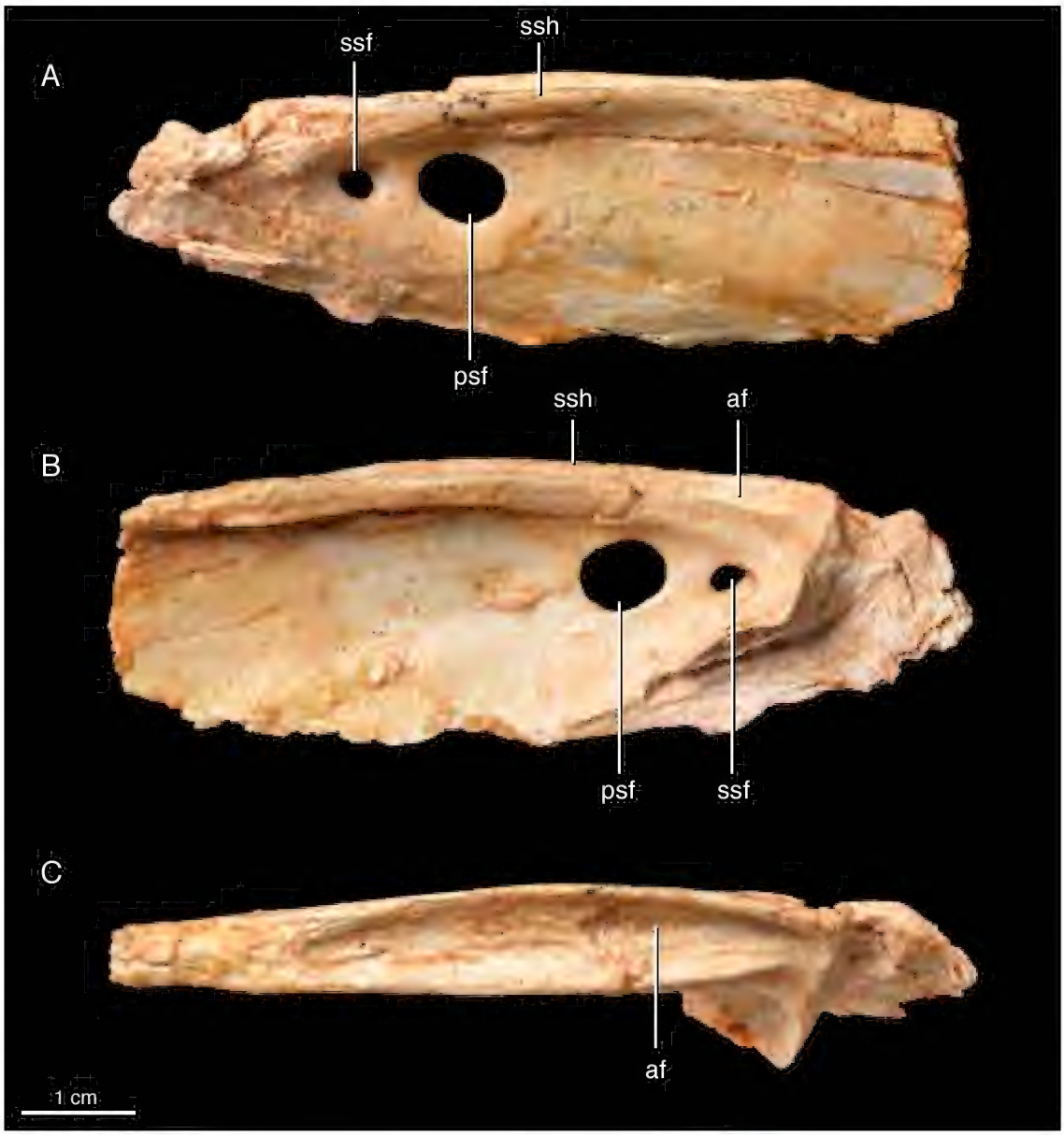

FIGURE 6. Right surangular of IGM 100/981 in **A,** lateral, **B,** medial, and **C,** dorsal views. Abbreviations: **af,** adductor fossa; **psf,** primary surangular foramen; **ssf,** secondary surangular foramen; **ssh,** surangular shelf.

the maxillary dentition of *Shanag ashile* (Turner et al., 2007c; Napoli et al., in review). There is no constriction or "waisting" between the root and crown, which are smoothly confluent as in all eudromaeosaurs but unlike in troodontids (Hendrickx et al., 2019). There are no prominent enamel ridges on the labial or lingual surfaces of the teeth. IGM 100/981 resembles *Dromaeosaurus albertensis* (Currie, 1995), *Atrociraptor marshalli* (Currie and Varricchio, 2004), and *Saurornitholestes langstoni* (Currie and Evans, 2019) but differs from most other eudromaeosaurs in having denticles on both the anterior and posterior carinae of the teeth. It further

resembles these taxa in that the denticles are markedly smaller on the anterior carina. While poor preservation makes the denticles impossible to observe on one or both carinae of several teeth, well-preserved carinae invariably preserve denticles, suggesting that all teeth were serrated on both sides in life. The anterior carina twists slightly labially moving apically along the tooth. This contrasts with the condition in *Dromaeosaurus albertensis*, in which the anterior carina is positioned on the lingual surface and twists toward the midline apically (Currie, 1995). The third dentary tooth is hypertrophied relative to the first and second teeth, similar to *Velociraptor mongoliensis* (IGM 100/982). CT imagery shows that it is near to life position, so this size difference is genuine, rather than the result of postmortem displacement, which is responsible for apparently large teeth in many dromaeosaurids. The partially erupted crown of the fourth dentary tooth as large as that of the third, making it likely that the mature tooth would have been comparable in size. While most of the middentary teeth are missing, it is clear that the posteriormost dentary teeth are smaller in size than those in the remainder of the toothrow, as in *Velociraptor mongoliensis* (AMNH FARB 6515) but unlike in troodontids, in which the posterior dentary teeth are generally larger than the anterior (Hendrickx et al., 2019).

Vertebrae

The vertebrae of IGM 100/981 are represented by fragments of cervical, dorsal, and caudal vertebrae. These include one anterior cervical, fragments of two midposterior cervicals, one partial posterior cervical, five anterior-middorsals, and five midposterior dorsals. Therefore, 14 individual presacral vertebrae are represented. The vertebrae are of varying quality of preservation and degree of preparation. CT imagery provides clarification of many details of their anatomy, as well as revealing a camellate internal structure like that of *Unenlagia*, *Velociraptor*, and *Itemirus*, but unlike the camarate structure of the dorsal vertebrae of *Saurornitholestes* (Gianechini and Zurriaguz, 2021).

The single preserved anterior cervical lacks its prezygapophyses and anterior and posterior articular surfaces. It compares favorably with C3 and C4 in *Tsaagan mangas* (IGM 100/1015) and *Shri devi* (IGM 100/980), so we tentatively identify it as C3/4. The centrum is strongly anterodorsally inclined, as is characteristic for dromaeosaurids (Ostrom, 1969b). The transverse processes are present as poorly developed projections. The postzygapophyseal facets face ventrally, as in *Shri devi* (IGM 100/980) but unlike *Tsaagan mangas* (IGM 100/1015), in which they face slightly posteroventrally, and no hyposphene is present. Like *Tsaagan mangas* (IGM 100/1015) but unlike *Shri devi* (IGM 100/980), the well-developed epipophyses do not extend farther posteriorly than the postzygapophyses. The ventral surface of the centrum is poorly exposed but appears to be gently convex, with no midline ridge or keel. The two midposterior cervicals (fig. 7) are preserved in articulation. While their position is difficult to assess without a complete vertebral series, their morphology is most consistent with C4–6 of *Tsaagan mangas*

FIGURE 7. Midcervical vertebrae of IGM 100/981 in **A,** dorsal and **B,** right lateral views. Abbreviations: **epi,** epipophysis; **ns,** neural spine; **poz,** postzygapophysis; **prz,** prezygapophysis; **tp,** transverse process.

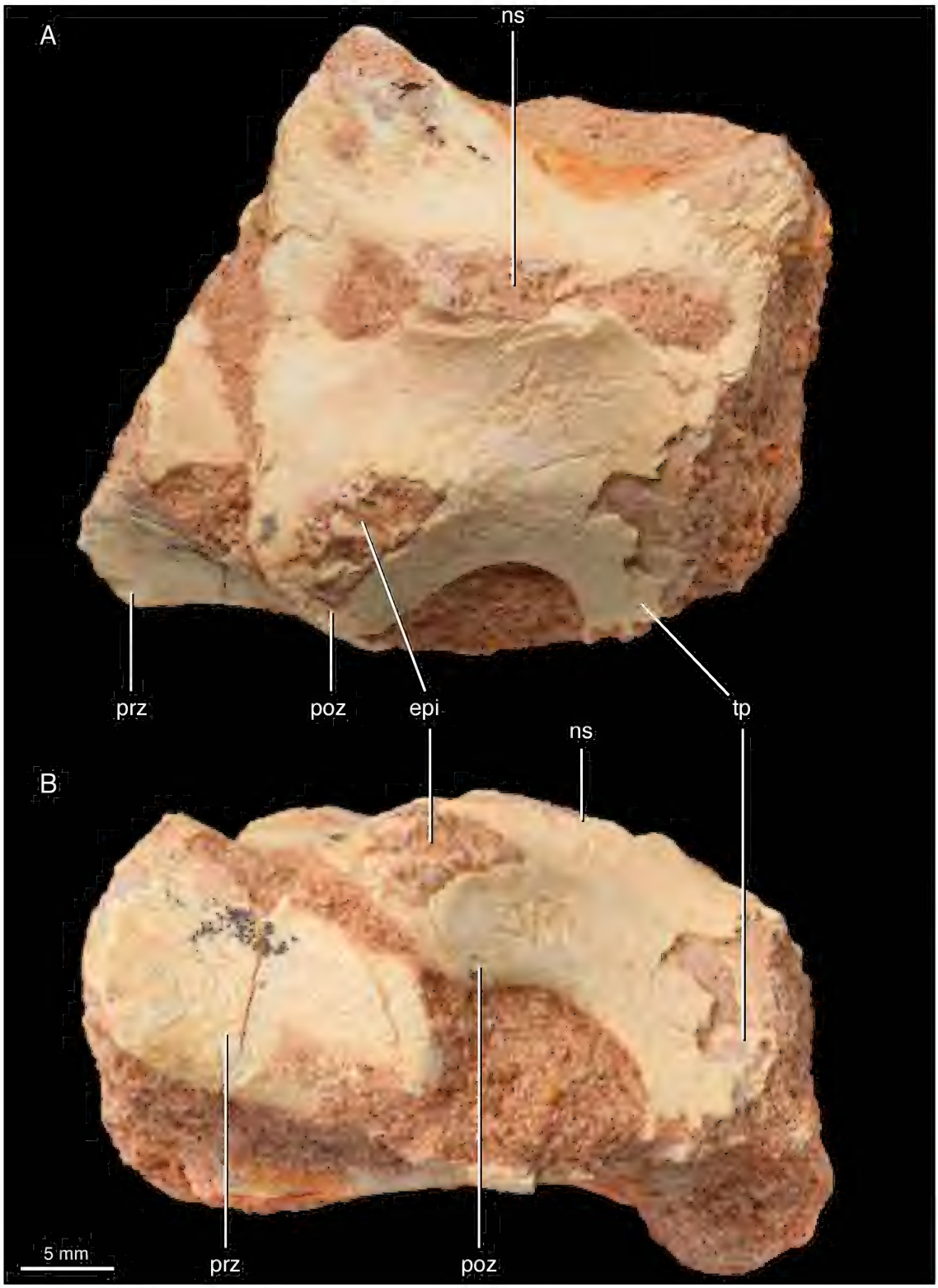
A
ns
prz
poz
epi
tp
B
ns
5 mm
prz
poz

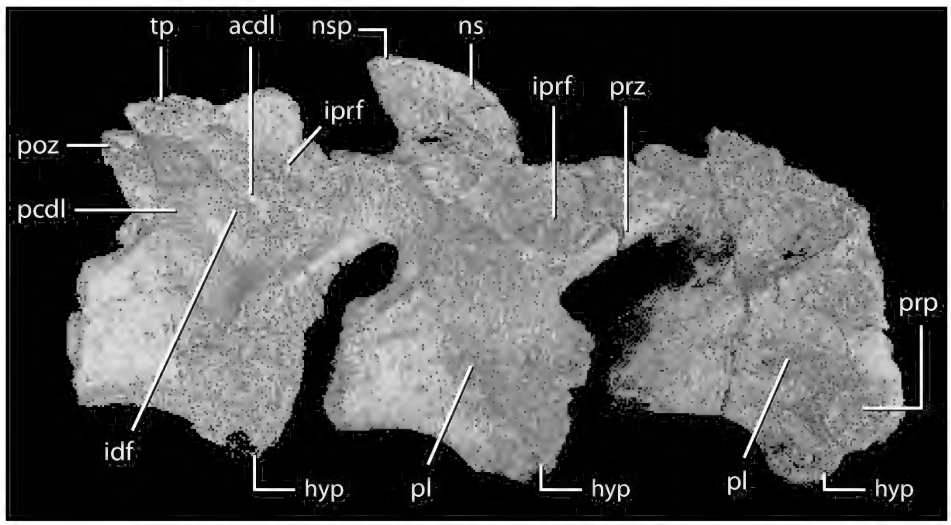

FIGURE 8. Digital rendering of D1–D3 of IGM 100/981 based on μCT imagery in left lateral view. Abbreviations: **acdl,** anterior centrodiapophyseal lamina; **hyp,** hypapophysis; **idf,** infradiapophyseal fossa; **iprf,** infraprezygapophyseal fossa; **ns,** neural spine; **nsp,** posterior extension of neural spine; **pcdl,** posterior centrodiapophyseal lamina; **pl,** pleurocoel; **poz,** postzygapophysis; **prp,** parapophysis; **prz,** prezygapophysis, **tp,** transverse process.

(IGM 100/1015) and *Shri devi* (IGM 100/980). The more anterior element is the more complete, missing its prezygapophyses and anterior articular surface, whereas the more posterior one is solely represented by a right prezygapophysis. The neural spine is broken, but it was anteroposteriorly broad and roughly centered on the neural arch. The neural canal opens anterodorsally, rather than strictly anteriorly as in both *Shri devi* (IGM 100/980) and *Tsaagan mangas* (IGM 100/1015). The epipophyses are low and more poorly developed than those of both *Shri devi* (IGM 100/980) and *Tsaagan mangas* (IGM 100/1015). The postzygapophyseal facets face posteroventrally, rather than strictly ventrally as in *Shri devi* (IGM 100/980) and *Tsaagan mangas* (IGM 100/1015). The ventral surface of the centrum is flat and smooth, with one ventrolaterally facing parapophysis visible at the anteroventral corner of the lateral surface of the centrum. As in eudromaeosaurs generally but unlike most other paravians, there are no traces of carotid processes. The single posterior cervical is poorly preserved, but is recognized by a keel on the ventral surface of the centrum, which is also found in the posteriormost cervical vertebrae of *Shri devi* (IGM 100/980) and *Tsaagan mangas* (IGM 100/1015).

Three anterior dorsals are preserved in articulation in a partially prepared block; rather than additional preparation, they were subjected to μCT scanning to visualize their morphology (fig. 8). All three vertebrae preserve hypapophyses, which are restricted to anterior dorsal vertebrae in deinonychosaurs (Gauthier, 1986). On this basis we identified these vertebrae as D1–D3. D2 preserves a complete neural spine, which is anteroposteriorly broad and low compared to the anterior dorsal neural spines of both *Shri devi* (IGM 100/980) and *Tsaagan mangas* (IGM 100/1015). Rather than the subtriangular profile common to the anterior dorsal neural spines of dromaeosaurids, the posterior margin projects posteriorly to form a distinctly con-

cave posterior margin, as in the neural spine of D6 in *Shri devi* (IGM 100/980). All three preserve hypapophyses at the anterior end of the centrum. These are short compared to the elongate hypapophyses of some oviraptorids, such as *Citipati osmolskae* (Napoli et al., in prep.), but similar in size to those of most pennaraptorans, including dromaeosaurids like *Shri devi* (IGM 100/980) and oviraptorosaurs such as *Nomingia gobiensis* (possibly a junior synonym of *Elmisaurus rarus*; see Funston et al., 2021) and *Khaan mckennai* (Barsbold et al., 2000; Balanoff and Norell, 2012). The transverse processes are poorly preserved but appear to be anteroposteriorly broad at their base, tapering toward their lateral extent. Anterior and ventral to the transverse processes, D2 and D3 clearly bear pneumatic fossae. Dorsal 3 has distinct infraprezygapophyseal and infradiapophyseal fossae, which are separated by a thin, almost transversely oriented anterior centrodiapophyseal lamina. This lamina is not present in D2, and it is unclear whether the one large pneumatic fossa simply represents the infraprezygapophyseal fossa or conjoined infraprezygapophyseal and infradiapophyseal fossae. Unlike *Shri devi* (IGM 100/980) but like most other theropods, D1–D3 have a single lateral pleurocoel on each side of the centrum; only the left side is observable in D1 and D2, but D3 preserves one pleurocoel on both the right and left. Unlike in most theropods, these pleurocoels are anteriorly displaced, with their posterior margin situated at approximately the anteroposterior midpoint of the centrum. Dorsal 4 is not articulated with the block containing D1–D3 (fig. 9). It has a smaller, less prominent hypapophysis, and is preserved in articulation with a partial middorsal (D5). Dorsal 4 displays clear infraprezygapophyseal and infradiapophyseal fossae, separated by a thin, posterodorsally inclined anterior centrodiapophyseal lamina. The posterior centrodiapophyseal lamina is much larger, but incomplete, and a potential infrapostzygapophyseal fossa is not exposed. The neural spine is taller than that of D2, but appears to have had a similar posterior projection at its dorsal end. The pleurocoel on the centrum of D4 is more strongly anteriorly displaced than those of the preceding vertebrae. Dorsal 5 is poorly exposed, but clearly shows the characteristic pediculate parapophysis of dromaeosaurids (Norell and Makovicky, 1997). The parapophysis appears to be below the level of the transverse process, unlike *Velociraptor mongoliensis* (IGM 100/986) but like *Shri devi* (IGM 100/980) and *Deinonychus antirrhopus* (Ostrom, 1969b; Turner et al., 2021). Dorsal 5 lacks a hypapophysis, but has a keeled ventral margin of the centrum.

Two midposterior dorsals are well preserved. Based on a general trend of centrum shortening, one can be confidently identified as more anterior, though its precise position in the vertebral column is difficult to determine (fig. 10). It is missing most its neural spine, and the neural arch is only exposed on the left side. The parapophyses are poorly preserved, but are clearly projected on pedicels as in D5. The vertebra preserves infraprezygapophyseal, infradiapophyseal, and infrapostzygapophyseal fossae, which are larger than those of D4. The centrum is spool shaped and ventrally rounded, lacking a midline keel. The vertebra clearly preserves a hyposphene on its left postzygapophysis, but the meeting (or lack thereof) of the contralateral hyposphene is unobservable. A subsequent midposterior dorsal is more completely prepared (fig. 11). Its parapophysis are laterally projected, but their pedicels are poorly developed. The infraprezygapophyseal, infradiapophyseal, and infrapostzygapophyseal fossae are present. The

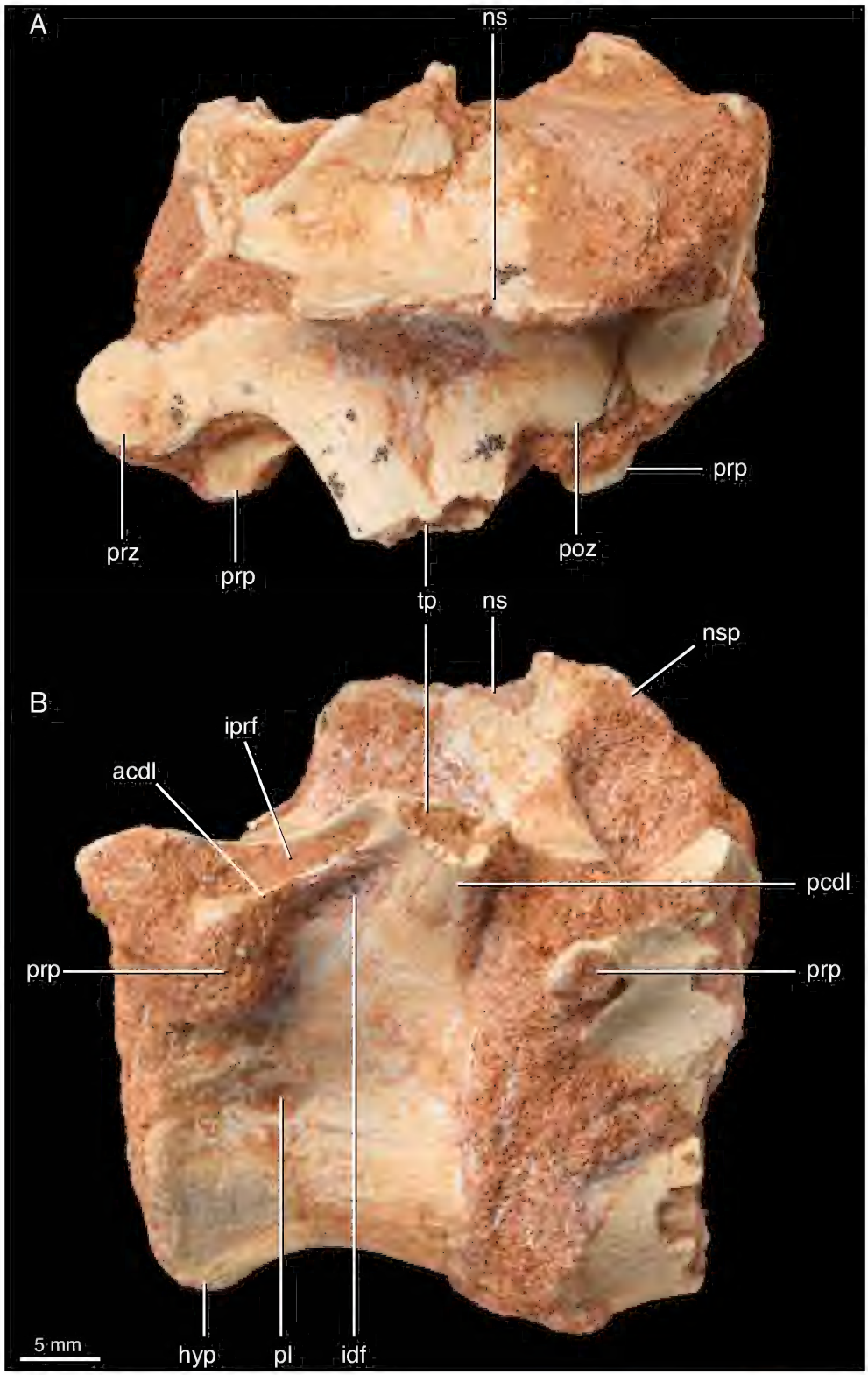
A
ns
prz
prp
poz
prp
tp
ns
nsp
B
iprf
acdl
pcdl
prp
prp
5 mm
hyp
pl
idf

hyposphenes do not meet on the midline but are connected by a web of bone, in contrast to the typical dromaeosaurid condition in which this web of bone is absent. The posteriormost dorsal has a proportionally elongate, rectangular neural spine, a relatively anteroposteriorly short centrum with large, slightly concave anterior and posterior articular surfaces (fig. 12). The hyposphenes on this vertebra are also joined by a web of bone.

Two caudal vertebrae, representing one anterior caudal and one distal caudal, are well preserved. The anterior caudal has a concave anterior articular surface and weakly concave posterior articular surface (fig. 13). The prezygapophyses are elongate, projecting approximately twice as far anterodorsally as the extent of the prezygapophyseal articular facets. There is a faint medial ridge between the prezygapophyses at the anterior margin of the neural arch, which continues posteriorly to become the anterior edge of the neural spine. The neural spine is recumbent and projects posterodorsally. The postzygapophyses are elongate anteroposteriorly, lack a hyposphene, and have ventrolaterally facing articular facets. The neural spine and postzygapophyses overhang the posterior margin of the centrum. The transverse processes project laterally and slightly posteriorly, and expand at their distal extent. The ventral surface of the centrum is marked by an hourglass-shaped sulcus, which is wide anteriorly and posteriorly but thin and faint at the anteroposterior midpoint. The centrum is three times as long anteroposteriorly as it is mediolaterally wide. Unlike in *Citipati osmolskae* (Napoli and Norell, in prep.) there is no trace of pneumatic foramina or fossae on this midcaudal. The posterior caudal (fig. 14) is less completely preserved, but a cast of a now-missing second posterior caudal is present, and preserves the missing pre- and postzygapophyses. The prezygapophyses are elongate, as is typical for eudromaeosaurs and exemplified by *Deinonychus antirrhopus* (Ostrom, 1969b) and *Velociraptor mongoliensis* (Norell and Makovicky, 1999). There is no trace of a neural spine, save for a faint ridge along the dorsal surface of the neural arch, which is continuous with a faint sulcus between the postzygapophyses, which are elongate and overhang the posterior extent of the centrum. The transverse processes are extremely reduced but discernable on the lateral face of the centrum, which is also three times as long as wide and bears an hourglass-shaped ventral sulcus.

Forelimb

The forelimb of IGM 100/981 is represented by fragments of humerus, radius, ulna, and part of the left manus. The distal ends of the right and left humeri are preserved, as well as a fragment of the proximal end of the right. Proximally, the right humerus exhibits a broken, but clearly small, deltopectoral crest (fig. 15). The lateral surface of the apex of the deltopectoral crest is rugose, and the medial surface is striated. The distal articular surfaces are damaged, but a distinct ectepicondyle is evident on both elements (fig. 16). Anteriorly, there is a well-

FIGURE 9. D4 and partial D5 of IGM 100/981 in **A,** dorsal and **B,** left lateral views. Abbreviations: **acdl,** anterior centrodiapophyseal lamina; **hyp,** hypapophysis; **idf,** infradiapophyseal fossa; **iprf,** infraprezygapophyseal fossa; **ns,** neural spine; **nsp,** posterior extension of neural spine; **pcdl,** posterior centrodiapophyseal lamina; **pl,** pleurocoel; **poz,** postzygapophysis; **prp,** parapophysis; **prz,** prezygapophysis, **tp,** transverse process.

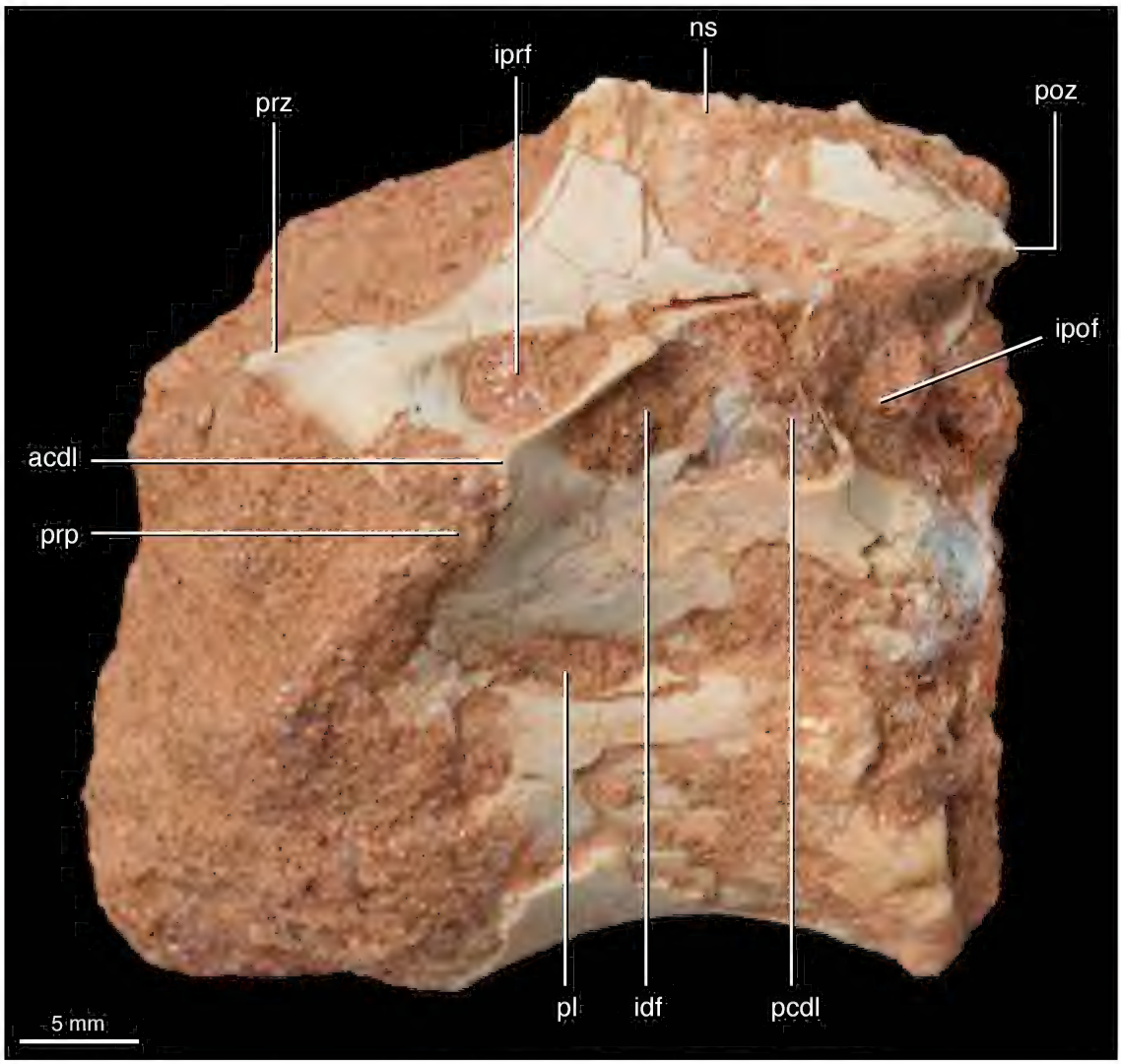

FIGURE 10. First preserved posterior dorsal of IGM 100/981 in left lateral view. Abbreviations: **acdl,** anterior centrodiapophyseal lamina; **idf,** infradiapophyseal fossa; **ipof,** infrapostzygapophyseal fossa; **iprf,** infraprezygapophyseal fossa; **ns,** neural spine; **pcdl,** posterior centrodiapophyseal lamina; **pl,** pleurocoel; **poz,** postzygapophysis; **prp,** parapophysis; **prz,** prezygapophysis.

developed fossa that likely corresponds to the fossa musculus brachialis (Baumel and Witmer, 1993) of modern birds. Posteriorly, there is a slightly concave fossa on the medial half of the element which may correspond to the sulcus humerotricipitalis of modern birds (Baumel and Witmer, 1993).

The proximal end of a right ulna and the proximal and distal ends of the right radius are preserved (fig. 17). The ulna has concave medial (= ventral) and a convex lateral (= dorsal) cotylae. As in all dromaeosaurids, the olecranon process is small and poorly developed. There is no indication of quill knobs along the posterior edge of the ulna, unlike in *Velociraptor mongoliensis* (Turner et al., 2007a). The coronoid process is just distal to the lateral cotyle. As in *Balaur bondoc*,

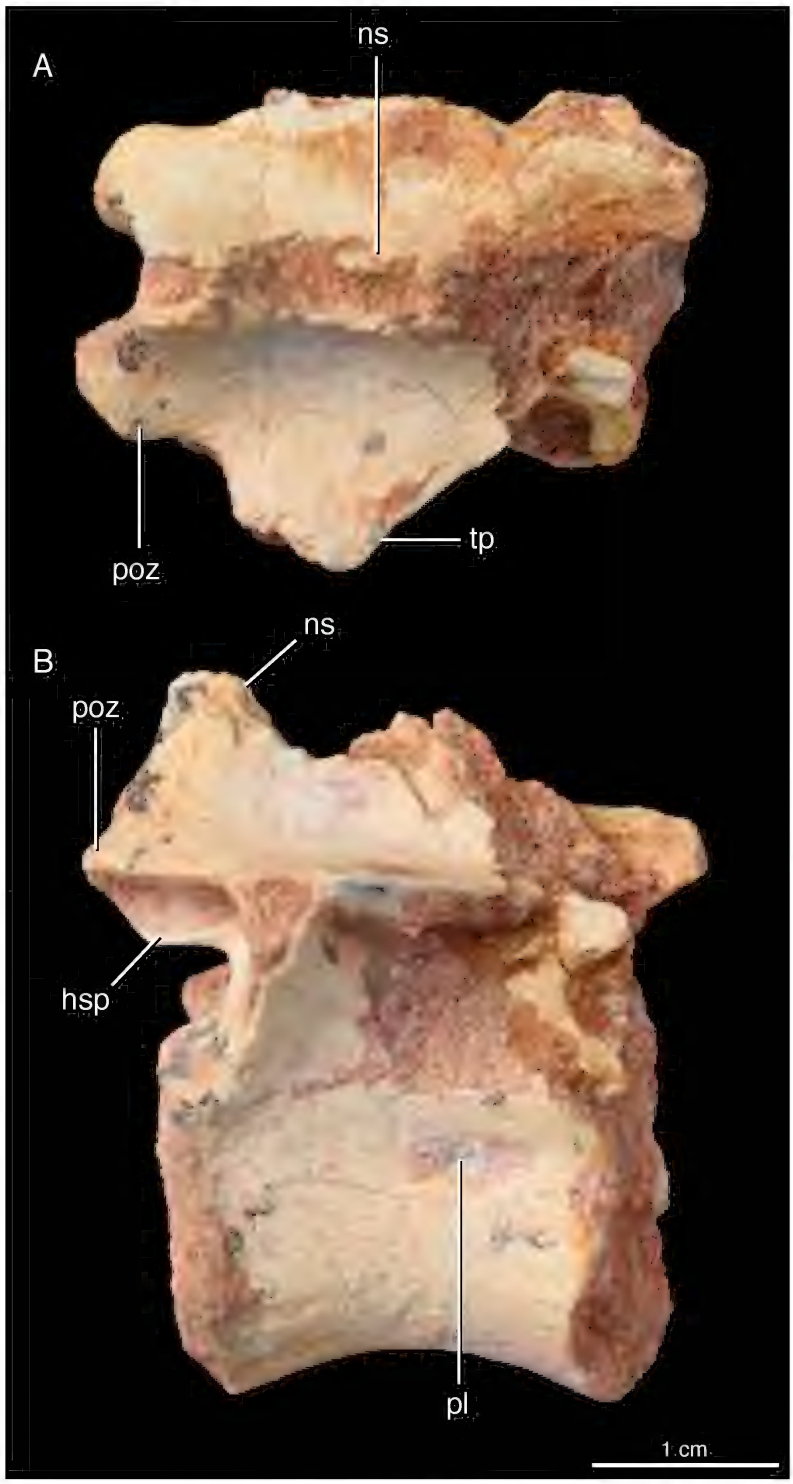

FIGURE 11. Middle preserved posterior dorsal of IGM 100/981 in **A,** dorsal and **B,** right lateral views. Abbreviations: **hsp,** hyposphene; **ns,** neural spine; **pl,** pleurocoel; **poz,** postzygapophysis; **tp,** transverse process.

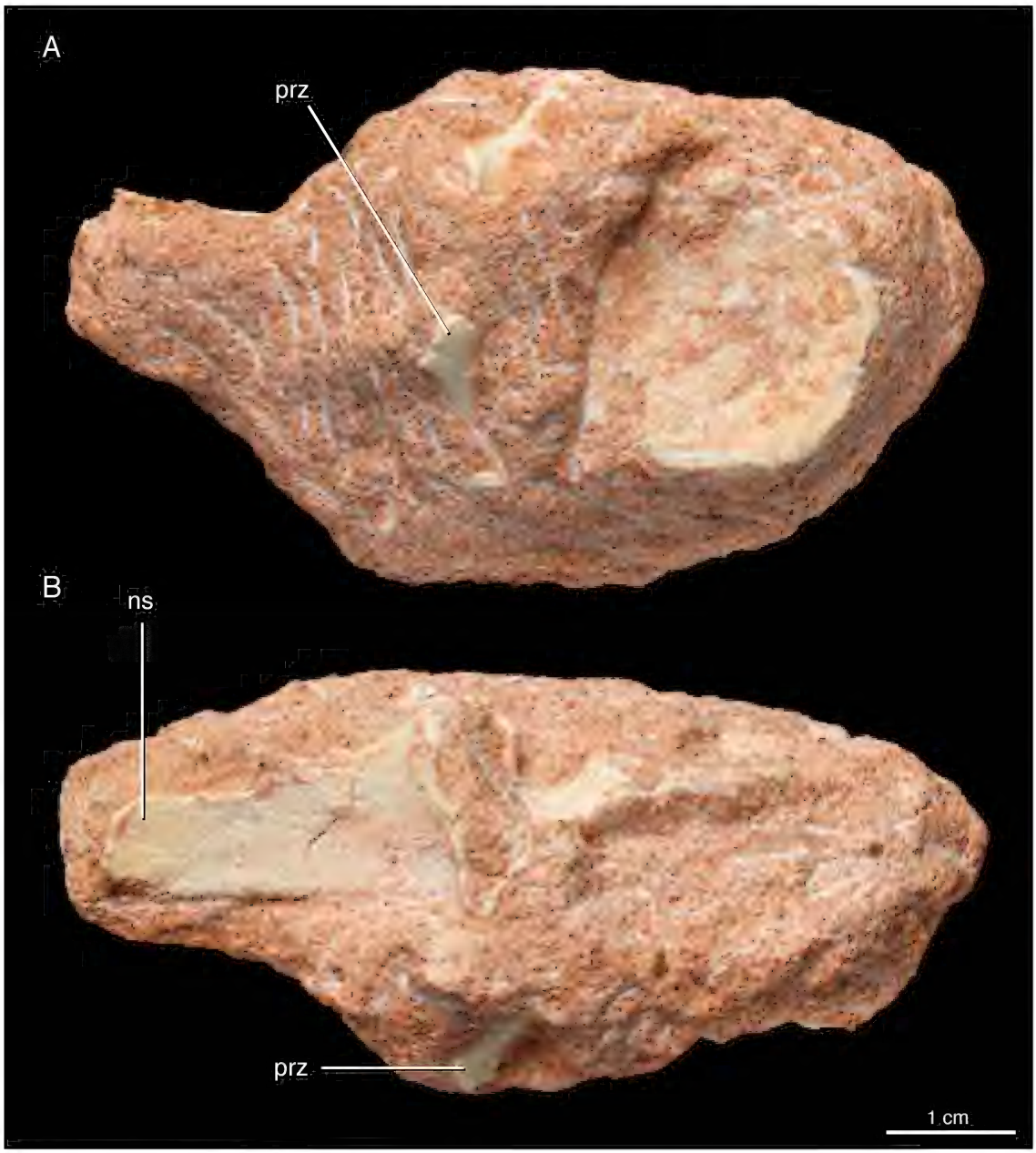

FIGURE 12. Last preserved posterior dorsal of IGM 100/981 in **A,** anterior and **B,** left lateral views. Dorsal is to the right in both panels. Abbreviations: **ns,** neural spine; **prz,** prezygapophysis.

a small ridge progresses distally from the coronoid process (Brusatte et al., 2013). The anterior surface of the ulna forms a subtriangular plane just distal to the cotylae, which is bounded by the ridge from the coronoid process and a ridge from the anterior margin of the medial cotyle. These ridges meet to form a keeled anterior margin of the ulna further distally, which is roughened and presumably functioned for soft-tissue attachment in life (possibly for the radioulnar syndesmo-

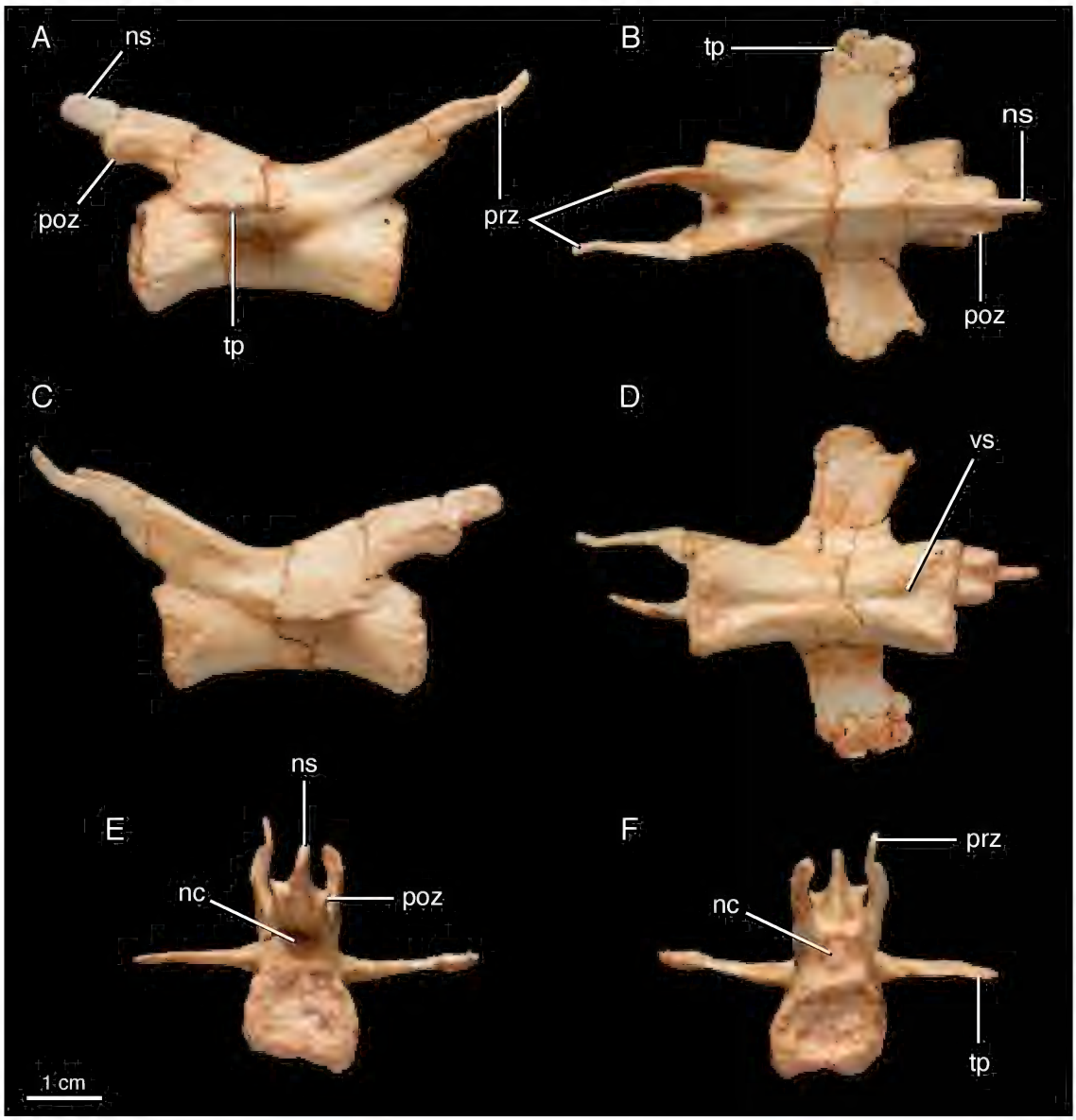

FIGURE 13. Anterior caudal vertebra of IGM 100/981 in **A,** right lateral, **B,** dorsal, **C,** left lateral, **D,** ventral, **E,** posterior, and **F,** anterior views. Abbreviations : **nc,** neural canal; **ns,** neural spine; **poz,** postzygapophysis, **prz,** prezygapophysis; **tp,** transverse process; **vs,** ventral sulcus.

sis). The radius preserves a flattened and expanded distal end, as in other pennaraptorans such as *Citipati osmolskae* (IGM 100/978; Napoli and Norell, in prep.; fig. 18).

The manus is represented a partial, articulated left carpus and metacarpus (fig. 19), and isolated phalanges. In all elements, the manual morphology corresponds closely to that of other dromaeosaurids such as *Velociraptor mongoliensis* (IGM 100/982), *Deinonychus antirrhopus* (Ostrom, 1969b), *Zhenyuanlong suni* (Lü and Brusatte, 2015), and *Microraptor zhaoianus* (Xu et al., 2003). The semilunate carpal is large and complete, capping most of metacarpal I and all

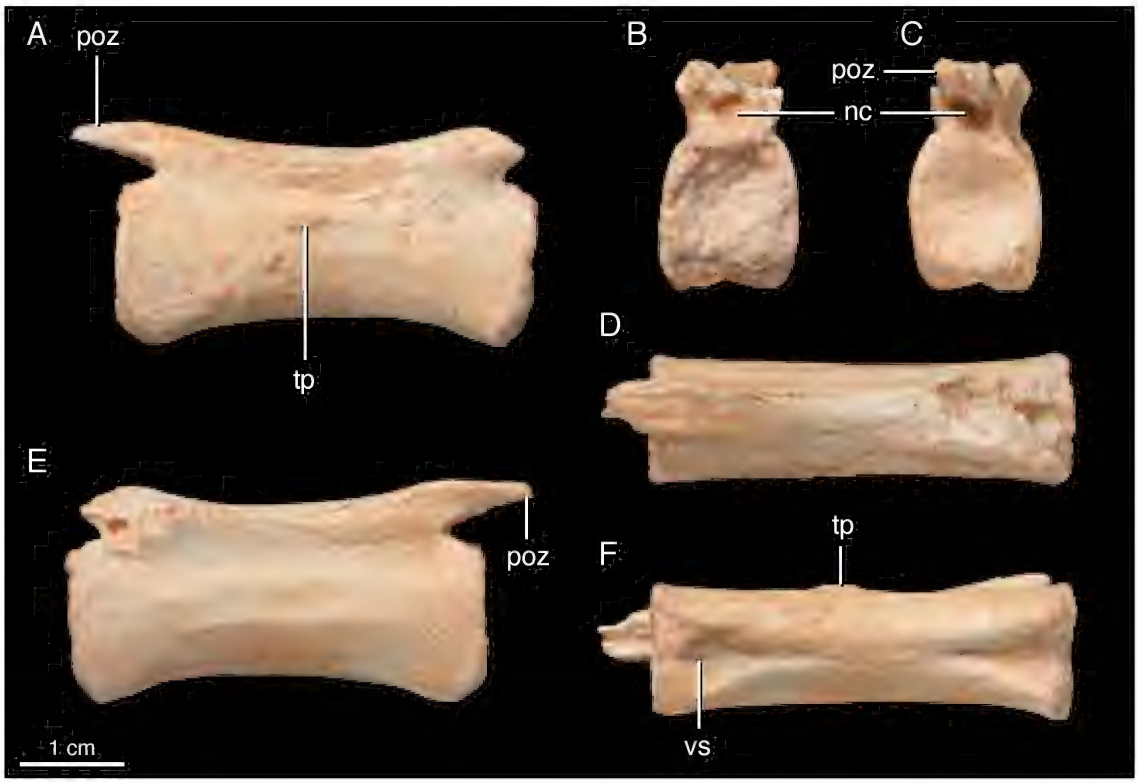

FIGURE 14. Posterior caudal vertebra of IGM 100/981 in **A,** right lateral, **B,** anterior, **C,** posterior, **D,** dorsal, **E,** left lateral, and **F,** ventral views. Abbreviations: **nc,** neural canal; **poz,** postzygapophysis; **tp,** transverse process; **vs,** ventral sulcus.

of metacarpal II. Metacarpal I is short and broad with a ginglymoid distal articular surface. Proximally metatarsal II is roughly as wide mediolaterally as is metacarpal I, but is missing its distal extent. The preserved proximal portion of metacarpal III is reduced to a thin splint and is affixed to the medial side of metacarpal II, as in most dromaeosaurids but unlike the proportionally robust metacarpal III of the microraptorine *Wulong bohaiensis* (Poust et al., 2020). While most phalanges are not confidently assignable, the right I-2, II-2, and II-3 phalanges are identified (figs. 20, 21). I-2 compares favorably to that of *Velociraptor mongoliensis* (IGM 100/982), albeit with a less strongly developed flexor tubercle. II-2 (fig. 20) resembles that of *Velociraptor mongoliensis* (IGM 100/982) as well, but with a weaker proximodorsal lip, larger and farther projecting proximoventral lip, and less deeply excavated collateral ligament pits. The proximodorsal lip of the ungual II-3 (fig. 21) is similarly less well developed in IGM 100/981 than in IGM 100/982.

Hind Limb

The ilium of IGM 100/981 is only represented by the left postacetabular process and ischiadic peduncle (fig. 22). The rim of the iliac blade is smooth, with no distinct tubercles or

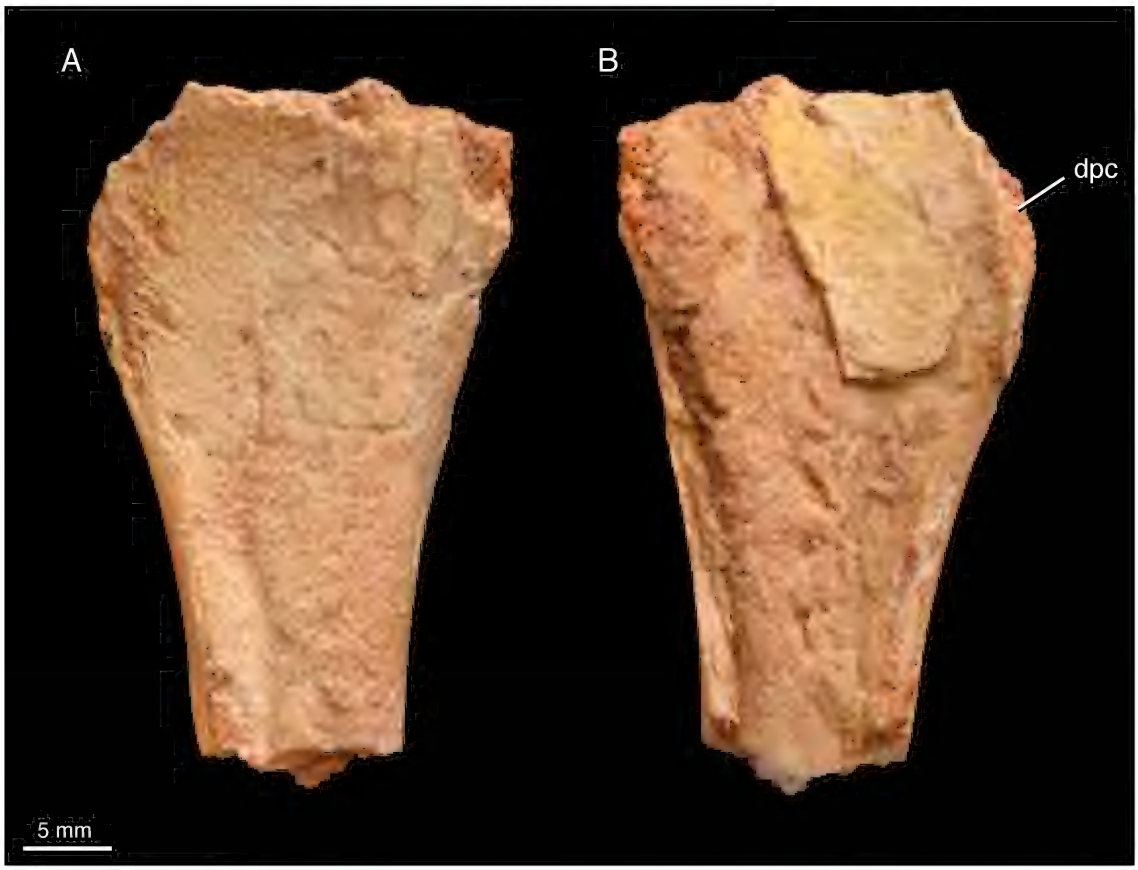

FIGURE 15. Proximal end of right humerus of IGM 100/981 in **A,** lateral and **B,** medial views. Abbreviation: **dpc,** deltopectoral crest.

rugosities. The postacetabular process is acuminate, rather than rounded or squared. The brevis fossa is not visible in lateral view. In overall morphology, the preserved portion of the ilium compares favorably with that of *Shri devi* (IGM 100/980) and *Velociraptor mongoliensis* (IGM 100/985; IGM 100/986). The pubis is represented by the distal ends of the right and left elements, with the left being more complete (fig. 23). Part of the pubic apron is preserved, arising from the anterior edge of the left pubic shaft. The pubic apron does not appear to have extended as far proximally as in *Shri devi* (IGM 100/980) or *Velociraptor mongoliensis* (IGM 100/985; Norell and Makovicky, 1997, 1999). The pubic boot is small, as in other dromaeosaurids, lacking a discrete anterior process and with only a small posterior process.

Both femora of IGM 100/981 are present. The right femur is well preserved (figs. 24, 25), whereas the left femur is broken into several fragments, missing its distal end, and generally poorly preserved. Its head and greater trochanter are eroded, and a small portion of its shaft is missing, but many informative details of the proximal and distal ends of the element are readily interpretable. As in *Velociraptor mongoliensis* (IGM 100/986), the femoral head is directed strictly medially in anterior and posterior view. In dorsal view, it is slightly more anteriorly directed than that of *Velociraptor mongoliensis* (IGM 100/986). There is no indication of a capi-

FIGURE 16. Distal end of right humerus of IGM 100/981 in **A,** posterior and **B,** anterior views.

tal ligament fovea. Posteriorly, there is a wide and deep groove passing distolaterally that grades into the neck of the femoral head. A similar groove is present in *Velociraptor mongoliensis* (IGM 100/986), in which it is narrower and partially enclosed proximomedially. It may also be present in *Shri devi* (IGM 100/980), but severe erosion of the proximal end of the femur in this specimen makes this ambiguous. The greater trochanter is not preserved, but the lesser trochanter is present. It is rounded in lateral view, and projects farther anteriorly than that of *Shri devi* (IGM 100/980) but not so far anteriorly as in *Velociraptor mongoliensis* (IGM 100/986). As in other dromaeosaurids, but unlike oviraptorids such as *Khaan mckennai* (Balanoff and Norell, 2012) and *Citipati osmolskae* (Napoli and Norell., in prep.), there is no nutrient foramen situated medial to the lesser trochanter on the anterior surface of the femur. As in *Velociraptor mongoliensis* (IGM 100/986), there is a ridge on the lateral surface of the femur that begins at the level of the lesser trochanter and progresses distally before grading into the femoral shaft. In IGM 100/981, this structure is inflated relative to that of *Velociraptor* (IGM 100/986), and lacks a distinct peak; however, it is less distinct than that of *Shri devi* (IGM 100/980). The femur lacks a distinct fourth trochanter, which is represented solely by a ridge on the posteromedial corner of the proximal femur. The ridgelike conformation of the fourth trochanter is similar to the more well-developed fourth trochanter in *Velociraptor mongoliensis* (IGM 100/986; Norell and Makovicky, 1999) and unlike that of *Shri devi* (IGM 100/980), in which it is present as a depression with rugose, raised sides (Turner et al., 2021). No nutrient foramen is present

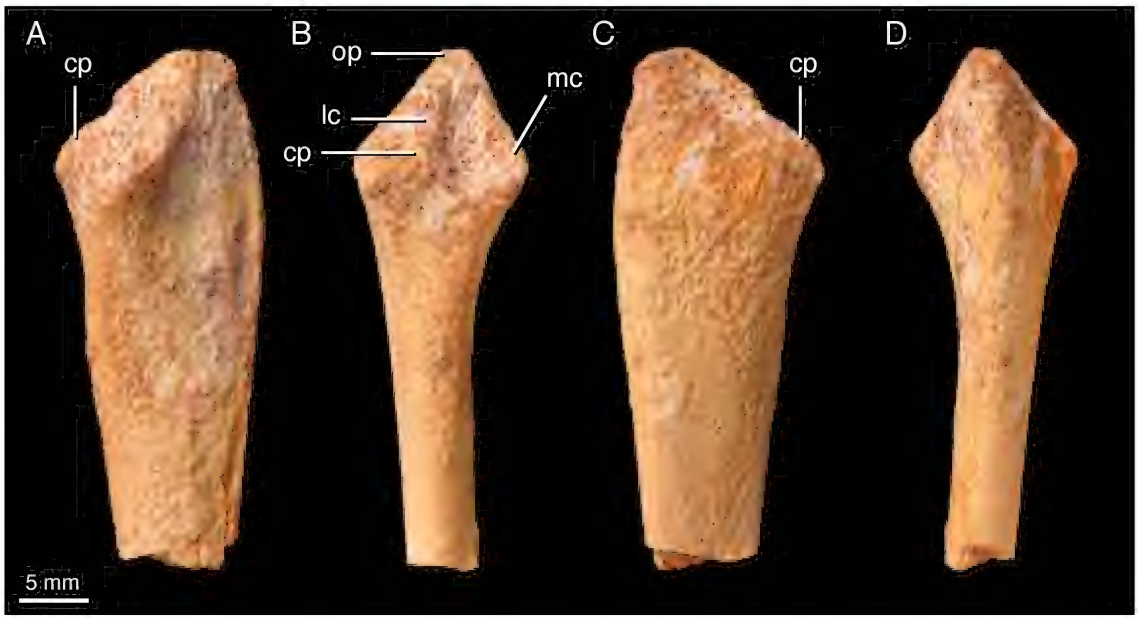

FIGURE 17. Proximal end of right ulna of IGM 100/981 in **A,** medial, **B,** anterior, **C,** lateral, and **D,** posterior views. Abbreviations: **cp,** coronoid process; **lc,** lateral cotyle; **mc,** medial cotyle; **op,** olecranon process.

on the posterior surface of the femur medial to the fourth trochanter, contrasting *Velociraptor mongoliensis* (IGM 100/986).

The lateral femoral condyle is mediolaterally wider than the medial condyle, which is strap-like in distal view, as in *Velociraptor mongoliensis* (IGM 100/986) but unlike *Shri devi* (IGM 100/980; fig. 25). The lateral condyle also extends slightly further distally than the medial, as in *Velociraptor mongoliensis*. The crista tibiofibularis forms a sulcus along its juncture with the femoral shaft on the lateral face of the bone, unlike both *Velociraptor mongoliensis* (IGM 100/986) and *Shri devi* (IGM 100/980), in which these surfaces grade into one another smoothly. At the distal extent of the crista tibiofibularis is a rounded ectocondylar tubercle, which is clearly demarcated from the lateral condyle and is laterally deflected, like in *Shri devi* (IGM 100/980) but unlike *Velociraptor mongoliensis* (IGM 100/986). The medial supracondylar ridge is poorly developed, and the popliteal fossa is more weakly excavated than in *Shri devi* (IGM 100/980), in which it is prominent and deep; however, it is more strongly developed than that of *Velociraptor mongoliensis* (IGM 100/986).

The proximal end of the left tibia (fig. 26) of IGM 100/981 is present, but so poorly preserved that it offers few recognizable morphological details. Both fibulae are missing. A partial left astragalus is preserved in association with left metatarsals II, III, and IV, which are poorly preserved (fig. 27). The astragalus is preserved in posterior view, with an incomplete ascending process. The proximal half of right metatarsal II, however, is well preserved and isolated (fig. 28), and the small right metatarsal I is also present (fig. 29). The right metatarsal I is almost complete, with a subtriangular, platelike proximal shaft that is roughened laterally for articulation with metatarsal II. The subtriangular profile of this surface is similar to that of oviraptorids such as

FIGURE 18. Distal end of right radius of IGM 100/981 in **A,** anterior and **B,** posterior views.

Citipati osmolskae (IGM 100/978; Napoli et al., in prep.) and *Shri devi* (IGM 100/980), but differs from *Velociraptor mongoliensis* (IGM 100/986) in which it is straplike with subparallel anterior and posterior edges. This articular surface ends just proximal to the distal head of metatarsal I, unlike in *Shri devi* (IGM 100/980), in which they are separated by nonarticular shaft. Metatarsal I of IGM 100/981 further differs from that of *Shri devi* (IGM 100/980) by its possession of a medial collateral ligament pit, and its deeply excavated lateral collateral ligament pit. Metatarsal II is markedly thinner than metatarsal III, as in *Velociraptor mongoliensis* (IGM 100/986) but unlike *Shri devi* (IGM 100/980), in which metatarsal II is apomorphically broad. Its lateral surface is flattened for articulation with metatarsal III. Proximally, there is a small tubercle along the posterior margin of the element, which is also found in *Velociraptor mongoliensis* (IGM 100/986). More distally, there is a raised, roughened eminence along the posteromedial shaft. This is in the same relative position as a distinct crest in *Velociraptor mongoliensis* (IGM 100/985; IGM 100/986) which is tentatively homologized with the medial plantar crest of modern birds (Norell and

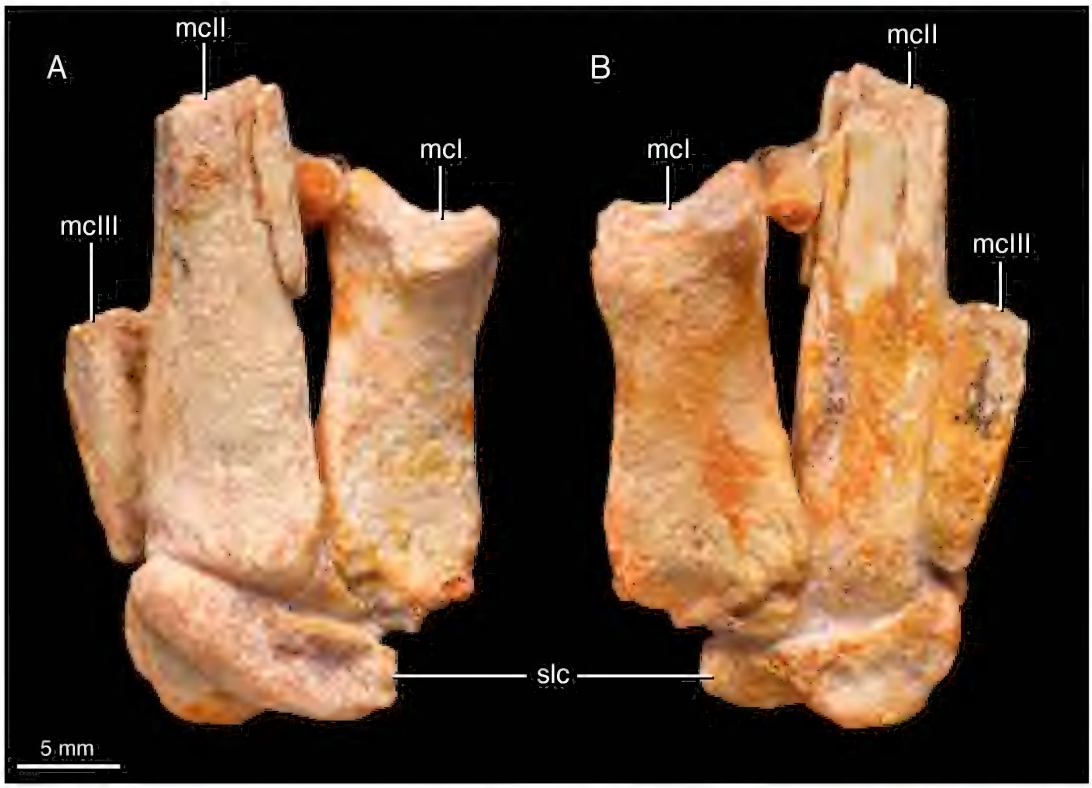

FIGURE 19. Left manus of IGM 100/981 in **A,** extensor and **B,** palmar views. Abbreviations: **mcI,** metacarpal I; **mcII,** metacarpal II; **mcIII,** metacarpal III; **slc,** semilunate carpal.

Makovicky, 1997); they likely represent the same structure. Both right and left metatarsal II are incomplete distally, but the proximal articular surface of phalanx II-1 indicates that it had a ginglymoid distal end, as is characteristic of dromaeosaurids.

The left metatarsus, which is poorly preserved but in articulation, illustrates several salient features. Left metatarsal IV is approximately 113 mm in proximodistal length, while the right femur is approximately 220 mm in proximodistal length. Although metatarsal III would have been the longest metatarsal, as in all theropods, the selected values allow a conservative estimate of metatarsus/femur length of 51%. This is substantially greater than that of both *Velociraptor mongoliensis* and *Shri devi*, in which the metatarsus is 35% and 44% the length of the femur, respectively. The metatarsus of IGM 100/981 therefore ranks among the longest known among dromaeosaurids, which generally have short metatarsals in relation to the length of their femur. Metatarsal III is visible in anterior view for the length of the metatarsus, which is therefore nonarctometatarsal. The distal articular surface of metatarsal III is missing, but the preserved proximal articular surface of phalanx III-1 indicates that it was ginglymoid in morphology. The distal articular surface of metatarsal IV is nonginglymoid, as in all theropods.

Sixteen pedal phalanges are present, comprising elements from digits I–IV on both sides; however, few digits are completely represented (figs. 30, 31). Digit I is represented by a small

FIGURE 20. Right phalanx II-2 of IGM 100/981 in **A,** medial and **B,** extensor views. Abbreviations: **clp,** collateral ligament pit; **pvl,** proximoventral lip.

ungual phalanx that is nearly identical to, but about three-quarters the size of, that of *Shri devi* (IGM 100/980). Digit II is represented by phalanges II-1, II-2, and II-3 on the left side, and phalanges II-2 and II-3 on the right. Left II-1 has a proximal articular surface with a strong anteroposterior ridge dividing it into medial and lateral cotyles, indicating that metatarsal II indeed had a ginglymoid distal articular surface. Its collateral ligament pits are deeply excavated, but it has only a weakly developed extensor tendon pit. II-2 is strongly modified for hyperextension with a distinct lobate flexor heel; it preserves very weak collateral ligament pits and lacks an extensor tendon pit. Neither right nor left II-3 preserves anything but their proximal end; however, these are about half the size of the hypertrophied phalanx II-3 of *Shri devi* (IGM 100/980), suggesting that this taxon had a relatively reduced "trenchant" second pedal ungual. Phalanx III-1 is the largest individual phalanx, with well-developed collateral ligament and extensor tendon pits that become weaker in successive phalanges in digit III. The proximal end of ungual III-4 is present and has a long, pointed anterodorsal lip with a weakly developed flexor tubercle. The phalanges of digit IV are smaller than those of digit III but are otherwise similar in morphology. Phalanx IV-1 lacks an anteroposterior ridge on its proximal articular surface, corresponding to the nonginglymoid distal articular surface of metatarsal IV.

PHYLOGENETIC ANALYSIS

To test the phylogenetic position of *Kuru kulla*, we scored IGM 100/981 in the most recent version of the Theropod Working Group (TWiG) matrix (Turner et al., 2021), which was modi-

FIGURE 21. Manual unguals of IGM 100/981 in **A, C,** lateral and **B, D,** medial views. Abbreviations: **I-2,** ungual phalanx I-2; **II-3,** ungual phalanx II-3.

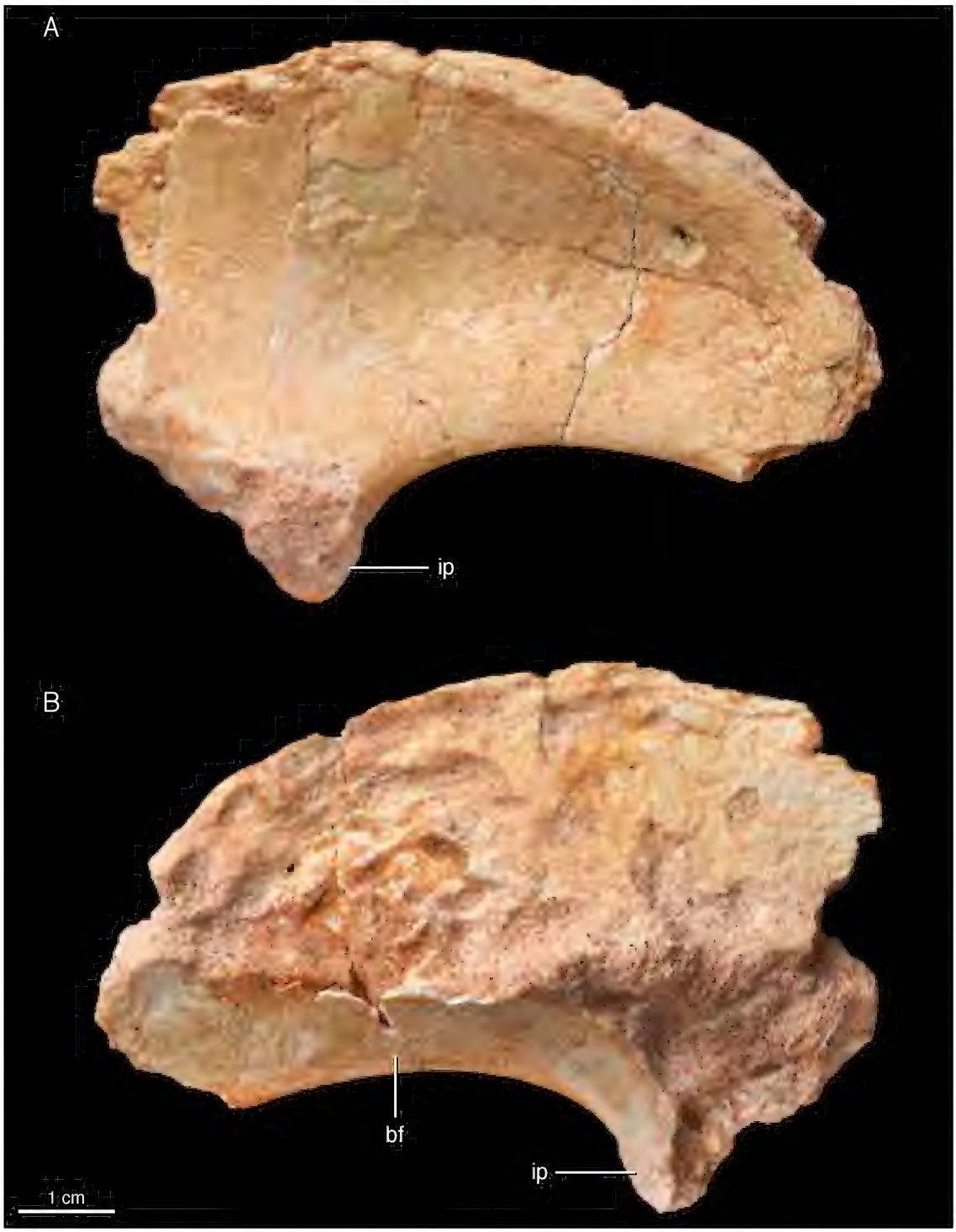

FIGURE 22. Left ilium of IGM 100/981 in **A,** lateral and **B,** medial views. Abbreviations: **bf,** brevis fossa; **ip,** ischiadic peduncle.

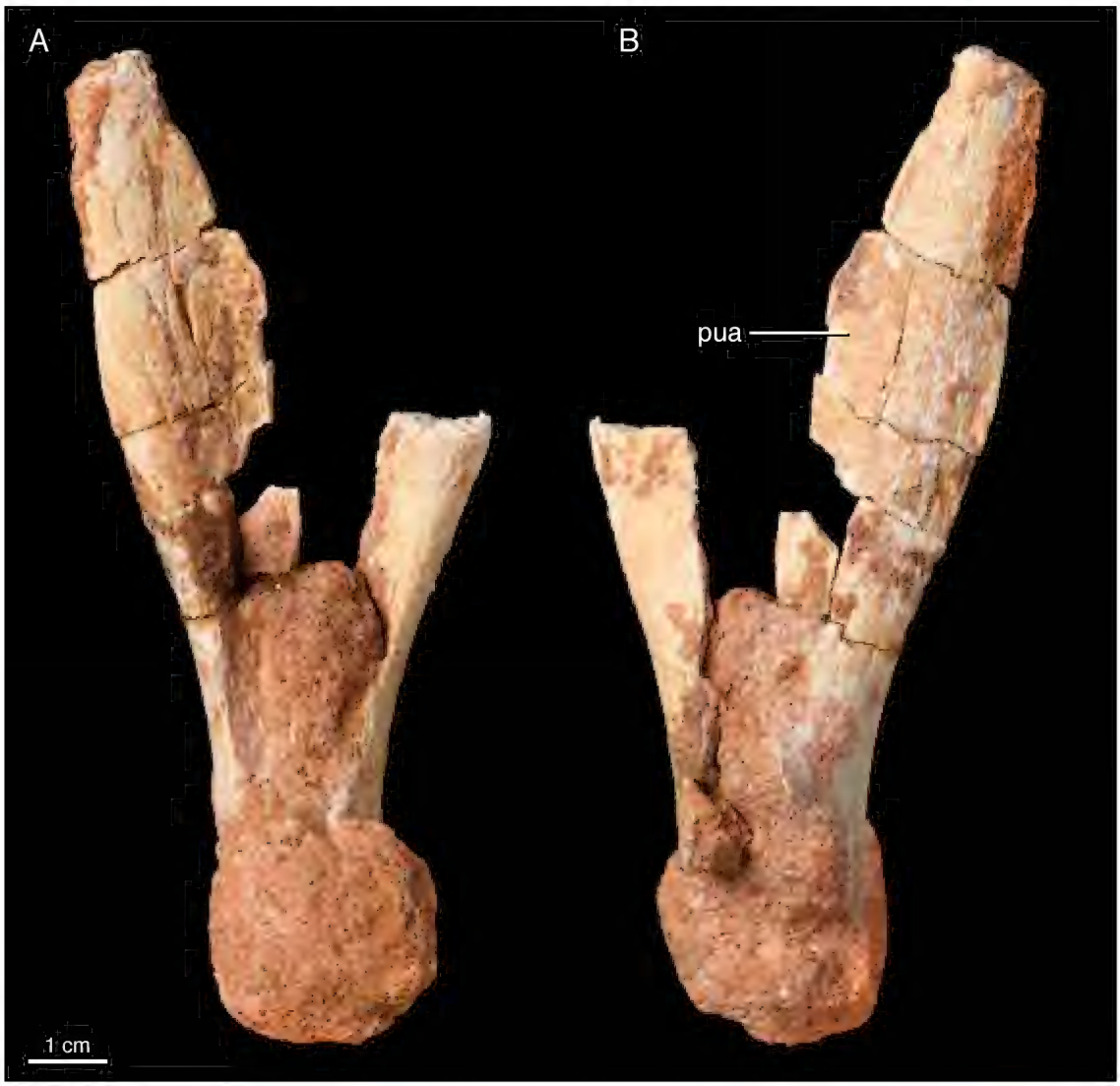

FIGURE 23. Pubis of IGM 100/981 in **A,** posterior and **B,** anterior views. Abbreviation: **pua,** pubic apron.

fied from Brusatte et al. (2014) and includes additional paravian observations for Pei et al. (2020). Several modifications were made to scorings of taxa already present in the matrix. *Adasaurus mongoliensis* was rescored to state 2 for character 72, describing its characteristically large surangular foramen. Firsthand reexamination of *Velociraptor mongoliensis* (IGM 100/982) and *Tsaagan mangas* (IGM 100/1015) found that they lacked a lip separating the ectopterygoid recess from the lateral temporal fenestra, and so they were newly scored as 0 for character 590. Following prior analyses of this dataset, we used equally weighted parsimony analysis implemented in TNT v. 1.5 (Goloboff et al., 2003; Goloboff and Catalano, 2016). We conducted multiple replications of new technology searches until 20 hits at the shortest length were achieved; the best trees obtained during this search were subjected to a final round of TBR

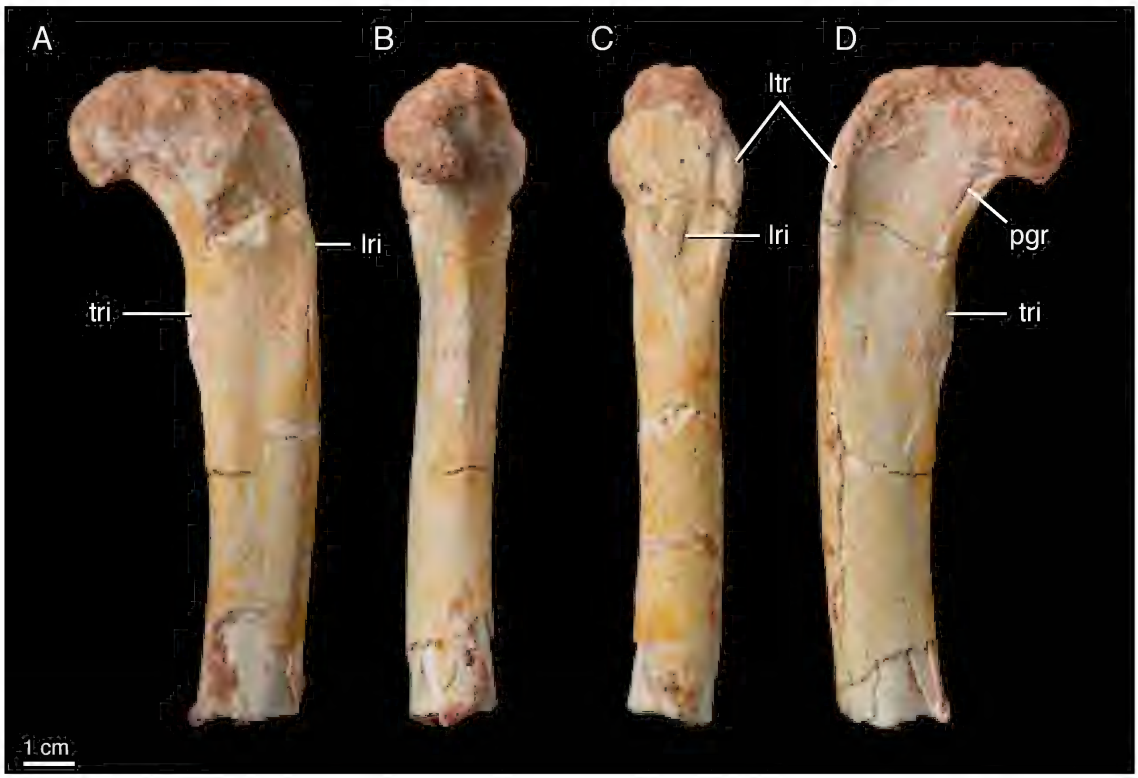

FIGURE 24. Proximal half of right femur of IGM 100/981 in **A,** anterior, **B,** medial, **C,** lateral, and **D,** posterior views. Abbreviations: **lri,** lateral ridge; **ltr,** lesser trochanter; **pgr,** posterior groove; **tri,** ridge homologous to the fourth trochanter.

branch swapping. Zero-length branches were collapsed, following rule 1 of Coddington and Scharff (1994). Dataset and supplementary files are available on MorphoBank (http://morphobank.org/permalink/?P4102).

This analysis resulted in 100,000 most parsimonious trees (memory overflowed) of 3411 steps (CI = 0.317, RI = 0.782, RC = 0.248). Bremer support values were calculated in TNT by holding 1000 trees that were between 1 and 9 steps longer than the most parsimonious trees, after which the bsupport command was run to assess which clades appeared at each suboptimal increment. Bremer support values of 9 should therefore be interpreted as "9 or more"; within Paraves, Bremer support is consistently low, so this does not obscure meaningful information. Jackknife support was calculated under a deletion probability of 0.20 with 1000 replicates.

A reduced strict consensus excluding the conflicting positions of a number of fragmentary dromaeosaurids (see TNT file on Morphobank) recovers *Kuru kulla* as the sister taxon to *Adasaurus mongoliensis* (fig. 32). Three characters optimize as synapomorphies of this relationship—a posterior surangular foramen that is ~30% the depth of the surangular (char. 72.2), absence of a fourth trochanter of the femur (char. 184.1), and thoracic centra that are markedly longer than their midpoint width (char. 312.1). The placement of *Kuru kulla* as sister to *Adasaurus mongoliensis* is supported by a Bremer value of 2 and a Jackknife frequency of 78. We note that these taxa further share a relatively reduced pedal digit II (in comparison to other eudro-

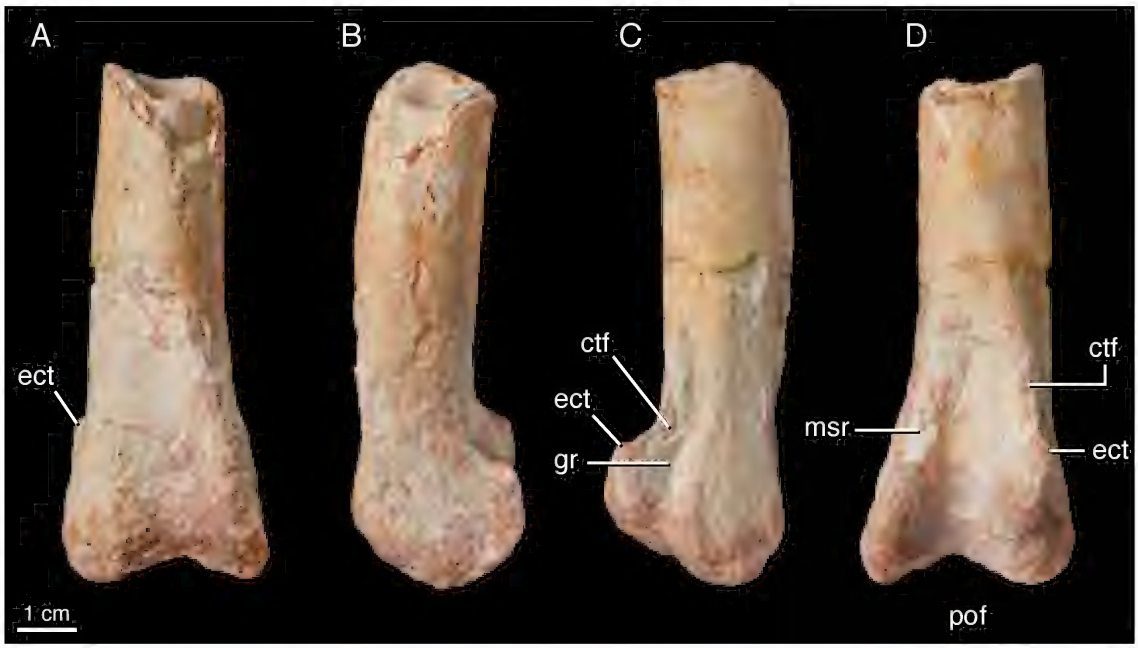

FIGURE 25. Distal half of right femur of IGM 100/981 in **A,** anterior, **B,** medial, **C,** lateral, and **D,** posterior views. Abbreviations: **ctf,** crista tibiofibularis; **ect,** ectocondylar tubercle; **gr,** groove formed by femoral shaft and crista tibiofibularis; **msr,** medial supracondylar ridge; **pof,** popliteal fossa.

maeosaurs), but that no character state in the TWiG matrix currently captures this morphology. We refrain from adding characters to the matrix at this time. However, we note that Bremer support throughout Paraves is quite low (seldom higher than 2, usually 1 or 0). Increased character sampling to resolve ingroup relationships within Paraves, especially within Dromaeosauridae, represents an important objective of future work.

DISCUSSION

Kuru kulla, the second velociraptorine eudromaeosaur reported from Khulsan, was apparently found only hours before the much more complete holotype specimen of *Shri devi*. The recognition of this taxon adds new detail to a recently proposed faunal structure for dromaeosaurid-bearing localities across the Gobi Desert—namely that the dromaeosaurid fauna at Gobi localities appeared to be characterized by the presence of distinct halszkaraptorine and velociraptorine dromaeosaurid taxa (Turner et al., 2021). *Kuru kulla* is the first velociraptorine dromaeosaurid to be described based on remains from a locality with a previously known velociraptorine taxon. It is impossible to directly compare the potential diets of these two species, as the skull and dentition of *Shri devi* are unknown, but given their close similarity in size and postcranial anatomy, and their close phylogenetic relationship, it seems likely that their diets were similar. It is unlikely that Khulsan was unique in its possession of two velociraptorine dromaeosaurids; indeed, the Zos Wash dromaeosaurid (IGM 100/3503) was found less than a kilometer from Ukhaa Tolgod and has a frontal that differs substantially from that of *Tsaagan*

FIGURE 26. Left tibia of IGM 100/981 in **A,** lateral and **B,** medial views.

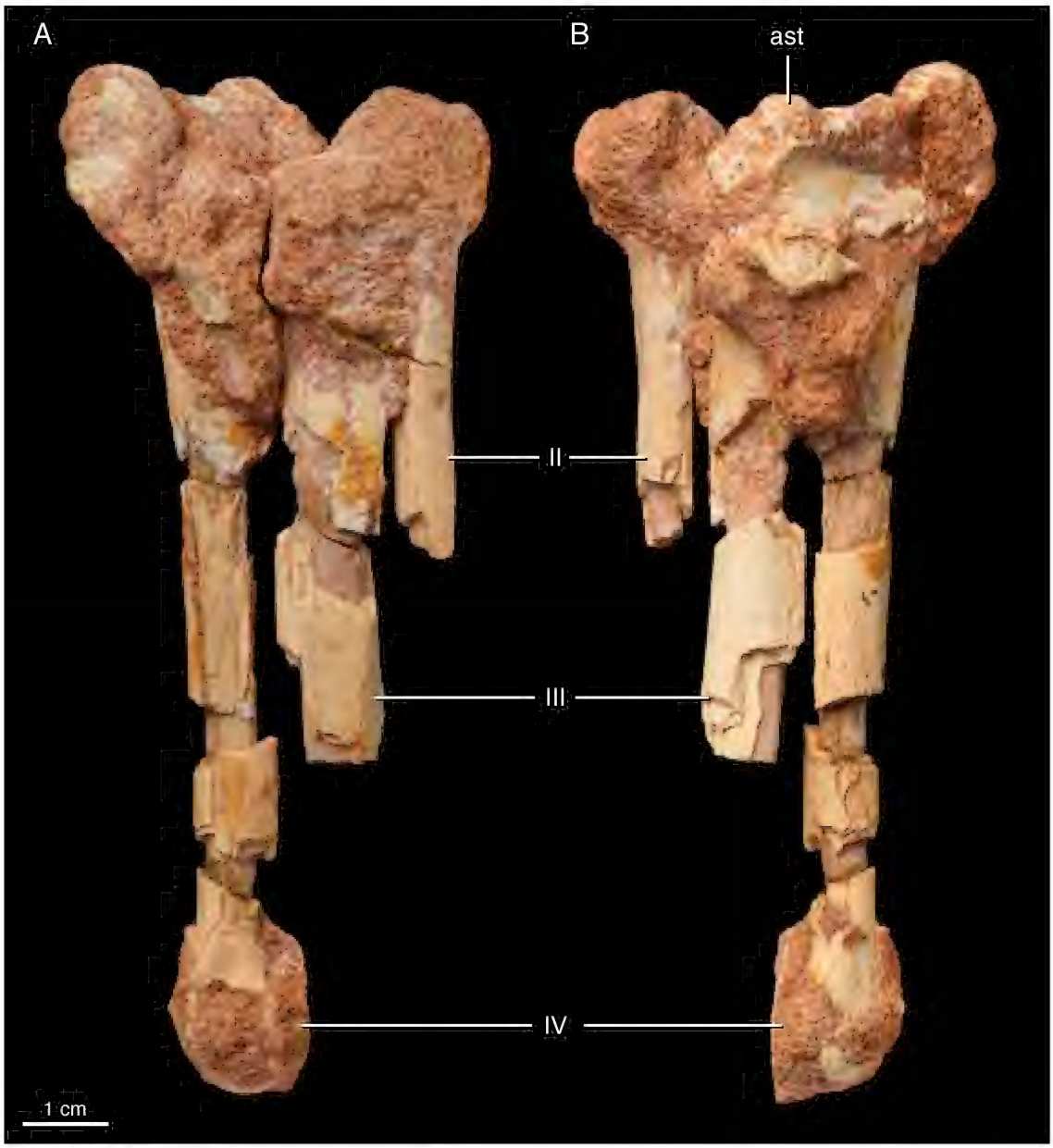

FIGURE 27. Left metatarsus of IGM 100/981 in **A,** posterior and **B,** anterior views. Abbreviations: **ast,** astragalus; **II;** metatarsal II; **III,** metatarsal III; **IV,** metatarsal IV.

FIGURE 28. Right metatarsal II of IGM 100/981 in **A,** medial and **B,** lateral views. Abbreviations : **mpc,** medial plantar crest; **tbl,** tubercle.

FIGURE 29. Right metatarsal I of IGM 100/981 in **A,** medial and **B,** lateral views.

mangas (Norell et al., 2006), the only described Ukhaa Tolgod dromaeosaurid. While the Zos Wash dromaeosaurid was provisionally referred to *Velociraptor mongoliensis* by Turner et al. (2007a), the specimen is currently under study and may prove to represent a distinct taxon; regardless, it is not referrable to *Tsaagan mangas*, and thus indicates that the fauna of Ukhaa Tolgod also had at least two velociraptorines present. At least one more eudromaeosaur specimen (ZPAL MgD-I/97) is known from Khulsan, which is currently referred to *Velociraptor mongoliensis* (Barsbold and Osmólska, 1999). This specimen clearly represents a taxon distinct from *Kuru kulla*, but whether it belongs to *Velociraptor mongoliensis*, *Shri devi*, or a third, yet unrecognized taxon remains to be seen. *Linheraptor exquisitus* and *Velociraptor osmolskae* are both known from the Wulansuhai Formation (Godefroit et al., 2008; Xu et al., 2010), but were found ~6 km apart, and are not confidently known to come from the same stratum; therefore,

FIGURE 30. Right pedal phalanges of IGM 100/981 in lateral view. Roman numerals denote digit number and Arabic the phalangeal position.

their potential coexistence cannot be established or rejected. There is little reason to assume a priori that we have recovered the maximum dromaeosaurid diversity from any of these localities, given their demonstrable richness at Khulsan and the general rarity of dromaeosaurid remains. Turner et al. (2021) noted that Ukhaa Tolgod, Tugrugyin Shireh, and Khulsan all hosted a single known velociraptorine that was distinct from those at the other two localities. *Kuru kulla* therefore adds to this faunal structure, and suggests that dromaeosaurid diversity in Cretaceous faunas was higher than previously appreciated (as predicted by Norell et al., 2006). As fieldwork and study of Gobi fossil material continues, it is possible that other Gobi localities will prove to have hosted multiple coexisting velociraptorines—whether the dromaeosaurid faunas of each locality remain distinct as more fossils are discovered will be important for assessing the mechanisms that led to the development of each locality's characteristic fauna.

The recognition of *Kuru kulla* as a distinct taxon from *Shri devi* with shared provenance has important implications for the taxonomic referral of newly discovered dinosaur material. It is often implicitly assumed that fossil-bearing localities or strata will yield a single species for each loosely defined "type" of animal, with competitive exclusion frequently invoked,

FIGURE 31. Left pedal phalanges of IGM 100/981 in lateral view. Roman numerals denote digit number and Arabic the phalangeal position.

without positive evidence, to justify this assumption (Molnar, 1990). As a result, all remains of animals belonging to particular clades (of varying levels of inclusivity) from a shared locality or formation are commonly referred to a single taxon unless stratigraphic separation can be demonstrated. For instance, Djadokhta-equivalent dromaeosaurid fossils were traditionally assigned to *Velociraptor mongoliensis* until the description of *Tsaagan mangas* (which was itself provisionally referred to *Velociraptor* for several years). It is possible that some workers would have ascribed the differences between IGM 100/981 and IGM 100/980 (the holotype of *Shri devi*) to intraspecific variation if fewer overlapping elements were known, especially given the shared provenance and close relationship of the two taxa. Had this been the case, *Shri devi* would have become an unrecognized chimera, which would have been an unknown confound in future studies. The recognition of *Kuru kulla* is important in demonstrating that the coexistence of closely related taxa with similar baupläne and body sizes was

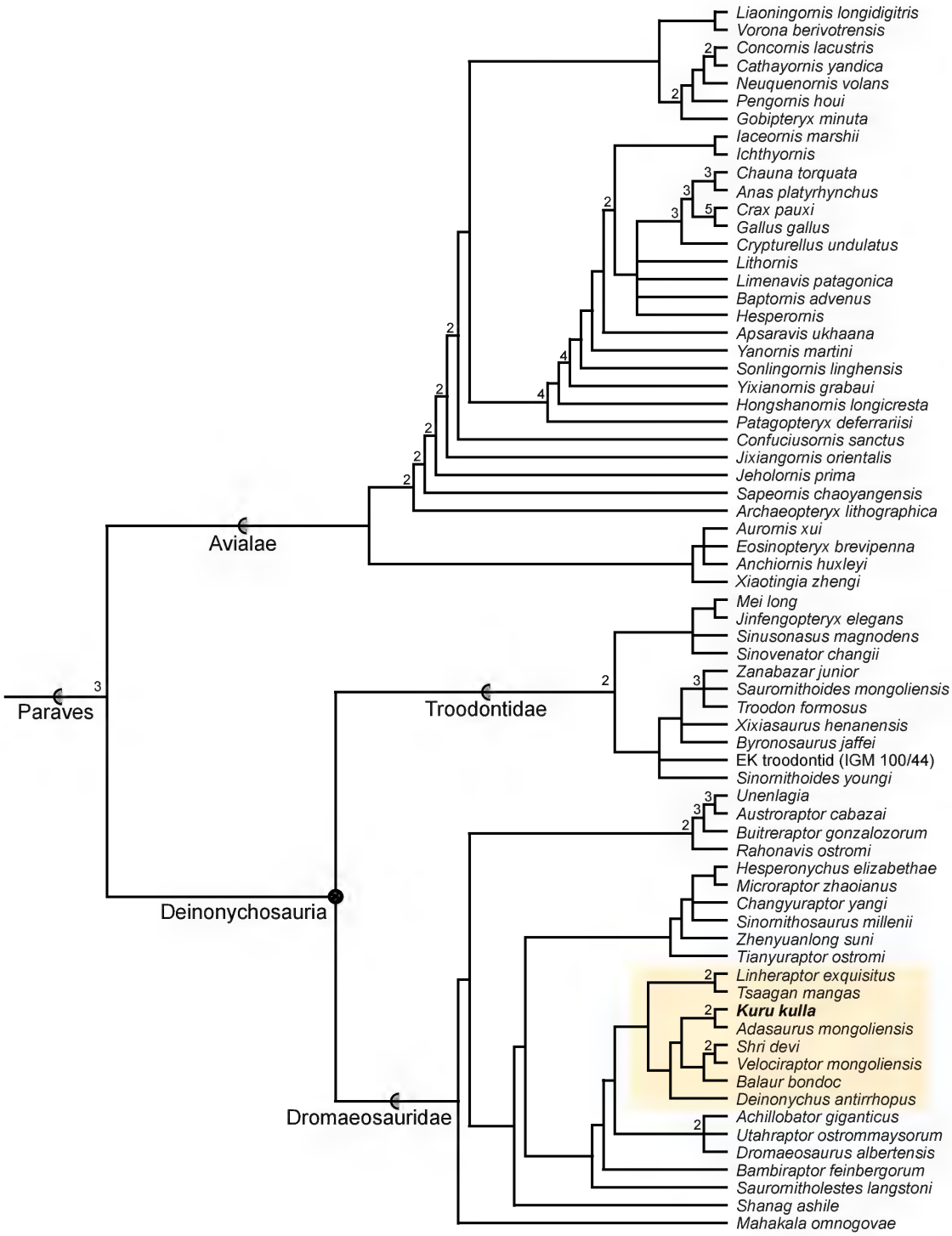

FIGURE 32. Phylogenetic position of *Kuru kulla* within Paraves. Reduced strict consensus of 100,000 most parsimonious trees (3411 steps, CI = 0.317, RI = 0.782, RC = 0.248), excluding several fragmentary dromaeosaurids. Bremer support is 1 unless noted. Highlight denotes Velociraptorinae.

a real phenomenon in nonavialan dinosaur faunas, just as it is in the modern day. As such, care must be taken when referring new material to known taxa—similarity and shared provenance are not necessarily sufficient justification for referral to an existing species, especially if the new specimen is fragmentary or missing its most diagnostic skeletal elements. We advocate an apomorphy-based approach to taxonomic referral, in which the apomorphies observable on a particular specimen justify its assignment to the least inclusive clade possible. This approach was pioneered by Norell (1989), and has recently been used in studies of Triassic archosauromorphs (Nesbitt et al., 2007; Nesbitt and Stocker, 2008). While apomorphy-based identification does not always allow for assignment at the species level (Bell et al., 2010), it is advantageous in that it does not assign specimens to a particular taxon unless there is positive evidence for its membership in that taxon, and therefore is unlikely to inadvertently create chimeric assemblages. Furthermore, future work quantifying the magnitude and distribution of intraspecific variation in extant taxa remains an important goal, as such data can provide crucial guidelines regarding which characters are most and least likely to be intraspecifically variable (and therefore, which are most reliable as justification for taxonomic separation). When comparisons to previously documented taxa from the same strata or locality are impossible due to nonoverlap of preserved elements, we recommend refraining from assigning the new specimen at the specific level until more material is available for comparison. A combination of paleontological fieldwork and continual taxonomic reappraisal is therefore of critical importance in building our understanding of the diversity evidenced by the fossil record.

SUMMARY

Kuru kulla is a new species of velociraptorine dromaeosaurid from the Barun Goyot Formation at Khulsan. It is the first velociraptorine to be recognized from a locality and stratum that has previously yielded a different velociraptorine species, in this case, the recently described *Shri devi* (Turner et al., 2021). As such, it provides important insight into the structure of Late Cretaceous nonavian dinosaur-bearing faunas. *Kuru kulla* demonstrates that similar, closely related dinosaur species could and did coexist, contrary to general expectations that such species would not tolerate each other due to competitive exclusion (Molnar, 1990). This has ramifications for the taxonomic referral of new fossil material and argues strongly for an apomorphy-based (rather than similarity- and provenance-based) approach to referral.

ACKNOWLEDGMENTS

We thank the members of the 1991 MAS-AMNH field crew for their efforts, which led to the discovery of IGM 100/981 and allowed this study to be conducted. The photographs comprising most of the figures in this paper were skillfully produced by Mick Ellison. IGM 100/981 was CT scanned at the AMNH Microscopy and Imaging Facility, and we thank Morgan Chase

and Andrew K. Smith for their help with scanning, reconstruction, and visualization. We further thank Lyn Merrill for surface scanning the majority of the specimen, Suzann Goldberg for her detective work regarding its curation, and Peter Makovicky for his insights on the Zos Wash material. The authors are indebted to Michael Pittman and an anonymous reviewer for their comments and feedback, which greatly improved the quality of the paper. J.G.N. and M.A.N. were funded by the Richard Gilder Graduate School, Newt and Calista Gingrich Endowment, and Macauley Family Endowment. Comparative data used in this study were collected by A.H.T. when supported by National Science Foundation award DEB 0608003.

REFERENCES

Balanoff, A.M., and M.A. Norell. 2012. Osteology of *Khaan mckennai* (Oviraptorosauria: Theropoda). Bulletin of the American Museum of Natural History 372: 1–77.

Barsbold, R. 1983. Carnivorous dinosaurs from the Cretaceous of Mongolia. Transactions of the Joint Soviet-Mongolian Paleontological Expedition 19: 5–119.

Barsbold, R., and H. Osmólska. 1999. The skull of *Velociraptor* (Theropoda) from the Late Cretaceous of Mongolia. Acta Paleontologica Polonica 44: 189–219.

Barsbold, R., H. Osmolska, M. Watabe, P.J. Currte, and K. Tsogtbaatar. 2000. A new oviraptorosaur (Dinosauria, Theropoda) from Mongolia: the first dinosaur with a pygostyle. Acta Palaeontologica Polonica 45: 97–106.

Baumel, J.J., and L.M. Witmer. 1993. Chapter 4. Osteologia. Handbook of avian anatomy: nomina anatomica avium: 45–132. Cambridge, MA: [Nuttall Ornithological Club].

Bell, C.J., J.A. Gauthier, and G.S. Bever. 2010. Covert biases, circularity, and apomorphies: a critical look at the North American Quaternary herpetofaunal stability hypothesis. Quaternary International 217 (1–2): 30–36.

Brusatte, S.L., et al. 2010. Tyrannosaur paleobiology: new research on ancient exemplar organisms. Science 329: 1481–1485.

Brusatte, S.L., et al. 2013. The osteology of *Balaur bondoc*, an island-dwelling dromaeosaurid (Dinosauria: Theropoda) from the Late Cretaceous of Romania. Bulletin of the American Museum of Natural History 374: 1–100.

Brusatte, S.L., G.T. Lloyd, S.C. Wang, and M.A. Norell. 2014. Gradual assembly of avian body plan culminated in rapid rates of evolution across the dinosaur-bird transition. Current Biology 24: 2386–2392.

Cau, A., et al. 2017. Synchrotron scanning reveals amphibious ecomorphology in a new clade of bird-like dinosaurs. Nature 552: 395–399.

Coddington, J., and N. Scharff. 1994. Problems with zero-length branches. Cladistics 10: 415–423.

Currie, P.J. 1995. New information on the anatomy and relationships of *Dromaeosaurus albertensis*. Journal of Vertebrate Paleontology 15: 576–5911.

Currie, P.J., and D.C. Evans. 2019. Cranial anatomy of new specimens of *Saurornitholestes langstoni* (Dinosauria, Theropoda, Dromaeosauridae) from the Dinosaur Park Formation (Campanian) of Alberta. Anatomical Record 303: 691–715.

Currie, P.J., and D.J. Varricchio. 2004. A new dromaeosaurid from the Horseshoe Canyon Formation (Upper Cretaceous) of Alberta, Canada. *In* P.J. Currie, E.B. Koppelhus, M.A. Shugar, and J.L. Wright (editors), Feathered dragons: 112–132. Bloomington, IN: Indiana University Press.

Dingus, L., et al. 2008. The geology of Ukhaa Tolgod (Djadokhta Formation, Upper Cretaceous, Nemegt Basin, Mongolia). American Museum Novitates 3616: 1–40.

Evans, D.C., D.W. Larson, and P.J. Currie. 2013. A new dromaeosaurid (Dinosauria: Theropoda) with Asian affinities from the latest Cretaceous of North America. Naturwissenschaften 100: 1041–1049.

Fanti, F., P.J. Currie, and D. Badamgarav. 2012. New specimens of *Nemegtomaia* from the Baruungoyot and Nemegt formations (Late Cretaceous) of Mongolia. PLoS One 7: e31330.

Funston, G.F., P.J. Currie, C. Tsogtbaatar, and T. Khishigjav. 2021. A partial oviraptorosaur skeleton suggests low caenagnathid diversity in the Late Cretaceous Nemegt Formation of Mongolia. PLoS One 16(7): e0254564.

Gauthier, J.A. 1986. Saurischian monophyly and the origin of birds. *In* K. Padian (editor), The origin of birds and the evolution of flight: 1–47. Berkeley, CA.

Gianechini, F.A., and V.L. Zurriaguz. 2021. Vertebral pneumaticity of the paravian theropod *Unenlagia comahuensis*, from the Upper Cretaceous of Patagonia, Argentina. Cretaceous Research 127: 104925.

Godefroit, P., P.J. Currie, L. Hong, C.Y. Shang, and Z.M. Dong. 2008. A new species of *Velociraptor* (Dinosauria: Dromaeosauridae) from the Upper Cretaceous of northern China. Journal of Vertebrate Paleontology 28: 432–438.

Goloboff, P.A., and S.A. Catalano. 2016. TNT version 1.5, with a full implementation of phylogenetic morphometrics. Cladistics 32: 221–238.

Goloboff, P.A., et al. 2003. Improvements to resampling measures of group support. Cladistics 19: 324–332.

Hendrickx, C., O. Mateus, and R. Araújo. 2015. A proposed terminology of theropod teeth (Dinosauria, Saurischia). Journal of Vertebrate Paleontology e982797-2: 1–18.

Hendrickx, C., O. Mateus, R. Araújo, and J. Choiniere. 2019. The distribution of dental features in non-avian theropod dinosaurs: taxonomic potential, degree of homoplasy, and major evolutionary trends. Palaeontologica Electronica 22.3.74: 1–110.

Li, R., et al. 2008. Behavioral and faunal implications of Early Cretaceous deinonychosaur trackways from China. Naturwissenschaften 95: 185–191.

Lü, J., and S.L. Brusatte. 2015. A large, short-armed, winged dromaeosaurid (Dinosauria: Theropoda) from the Early Cretaceous of China and its implications for feather evolution. Scientific Reports 5: 1–11.

Makovicky, P.J., S. Apesteguía, and F.L. Agnolín. 2005. The earliest dromaeosaurid theropod from South America. Nature 437: 1007–1011.

Maxwell, W.D., and J.H. Ostrom. 1995. Taphonomy and paleobiological implications of *Tenontosaurus-Deinonychus* associations. Journal of Vertebrate Paleontology 15: 707–712.

Molnar, R.E. 1990. Variation in theory and in theropods. *In* K. Carpenter and P.J. Currie (editors), Dinosaur systematics: approaches and perspectives: 71–79. Melbourne: Cambridge University Press.

Napoli, J.G., and M.A. Norell. In prep. Osteology and myology of *Citipati osmolskae*.

Napoli, J.G., B-A.S. Bhullar, S-C. Chang, M. Fabbri, A.H. Turner, and M.A. Norell. In review. Bird-eating stage in dromaeosaurid dinosaur evolution.

Nesbitt, S.J., and M.R. Stocker. 2008. The vertebrate assemblage of the Late Triassic Canjilon Quarry (northern New Mexico , USA), and the importance of apomorphy-based assemblage comparisons. Journal of Vertebrate Paleontology 28: 1063–1072.

Nesbitt, S.J., R.B. Irmis, and W.G. Parker. 2007. A critical re-evaluation of the late triassic dinosaur taxa of North America. Journal of Systematic Palaeontology 5: 209–243.

Norell, M.A. 1989. Late Cenozoic lizards of the Anza Borrego Desert, California. Natural History Museum of Los Angeles County Contributions in Science 414: 1–31.

Norell, M.A., and P.J. Makovicky. 1997. Important features of the dromaeosaur skeleton: information from a new specimen. American Museum Novitates 3215: 1–28.

Norell, M.A., and P.J. Makovicky. 1999. Important features of the dromaeosaurid skeleton II: information from newly collected specimens of *Velociraptor mongoliensis*. American Museum Novitates 3282: 1–45.

Norell, M.A., et al. 2006. A new dromaeosaurid theropod from Ukhaa Tolgod (Ömnögov, Mongolia). American Museum Novitates 3545: 1–51.

Osborn, H.F. 1924. Three new Theropoda, Protoceratops zone, Central Mongolia. American Museum Novitates 144: 1–12.

Osmólska, H. 1996. An unusual theropod dinosaur from the Late Cretaceous Nemegt Formation of Mongolia. Acta Palaeontologica Polonica 41: 1–38.

Ostrom, J.H. 1969a. A new theropod dinosaur from the Lower Cretaceous of Montana. Postilla 128: 1–17.

Ostrom, J.H. 1969b. Osteology of *Deinonychus antirrhopus*, an unusual theropod from the Lower Cretaceous of Montana. Peabody Museum of Natural History Bulletin 30: 1–165.

Pei, R., et al. 2020. Potential for powered flight neared by most close avialan relatives, but few crossed its thresholds. Current Biology 30: 1–14.

Perle, A., M.A. Norell, and J.M. Clark. 1999. A new maniraptoran theropod—*Achillobator giganticus* (Dromaeosauridae)—from the Upper Cretaceous of Burkhant, Mongolia. Contributions from the Geology and Mineralogy Chair, National Museum of Mongolia 1–105.

Pittman M., et al. 2020. The fossil record of Mesozoic and Paleocene pennaraptorans. *In* M. Pittman and X. Xu (editors), Pennaraptoran dinosaurs: past progress and new frontiers. Bulletin of the American Museum of Natural History 440: 37–95.

Poust, A.W., C. Gao, D.J. Varricchio, J. Wu, and F. Zhang. 2020. A new microraptorine theropod from the Jehol Biota and growth in early dromaeosaurids. Anatomical Record 303: 963–987.

Russell, D.A., and Z-M. Dong. 1993. A nearly complete skeleton of a new troodontid dinosaur from the early Cretaceous of the Ordos Basin, Inner Mongolia, People's Republic of China. Canadian Journal of Earth Sciences 30: 2163–2173.

Turner, A.H., P.J. Makovicky, and M.A. Norell. 2007a. Feather quill knobs in the dinosaur *Velociraptor*. Science 317: 1721.

Turner, A.H., D. Pol, J.A. Clarke, G.M. Erickson, and M.A. Norell. 2007b. A basal dromaeosaurid and size evolution preceding avian flight. Science 317: 1378–1381.

Turner, A.H., S.H. Hwang, and M.A. Norell. 2007c. A small derived theropod from Öösh, Early Cretaceous, Baykhangor Mongolia. American Museum Novitates 3557: 1–27.

Turner, A.H., P.J. Makovicky, and M.A. Norell. 2012. A review of dromaeosaurid systematics and paravian phylogeny. Bulletin of the American Museum of Natural History 371: 1–206.

Turner, A.H., S. Montanari, and M.A. Norell. 2021. A new dromaeosaurid from the Late Cretaceous Khulsan locality of Mongolia. American Museum Novitates 3965: 1–46.

Xu, X., X.L. Wang, and X.C. Wu. 1999. A dromaeosaurid dinosaur with a filamentous integument from the Yixian Formation of China. Nature 401: 262–266.

Xu, X., Z. Zhou, and X. Wang. 2000. The smallest known non-avian theropod dinosaur. Nature 408: 705–708.

Xu, X., et al. 2003. Four-winged dinosaurs from China. Nature 421: 335–340.

Xu, X., et al. 2010. A new dromaeosaurid (Dinosauria: Theropoda) from the Upper Cretaceous. Zootaxa 2403: 1–9.

Xu, X., et al. 2015. The taxonomic status of the Late Cretaceous dromaeosaurid *Linheraptor exquisitus* and its implications for dromaeosaurid systematics. Vertebrata PalAsiatica 53: 29–62.

Yi, H-Y., and M.A. Norell. 2013. New materials of *Estesia mongoliensis* (Squamata: Anguimorpha) and the evolution of venom grooves in lizards. American Museum Novitates 3767: 1–31.

All issues of *Novitates* and *Bulletin* are available on the web (https://digitallibrary.amnh.org/handle/2246/5). Order printed copies on the web from:

https://shop.amnh.org/books/scientific-publications.html

or via standard mail from:

American Museum of Natural History—Scientific Publications
Central Park West at 79th Street
New York, NY 10024

♾ This paper meets the requirements of ANSI/NISO Z39.48-1992 (permanence of paper).